1971-06

Heat transfer analysis of a radio frequency brain probe.

Gengler, Patrick Lee

HEAT TRANSFER ANALYSIS
OF A
RADIO-FREQUENCY BRAIN PROBE

Patrick Lee Gengler

United States
Naval Postgraduate School

THESIS

HEAT TRANSFER ANALYSIS OF A
RADIO-FREQUENCY BRAIN PROBE

by

Patrick Lee Gengler

Thesis Advisor: T. E. Cooper

June 1971

Approved for public release; distribution unlimited.

Heat Transfer Analysis of a Radio-Frequency Brain Probe

by

Patrick Lee Gengler
Ensign, United States Navy
B.S., Marquette University, 1970

Submitted in partial fulfillment of the
requirements for the degree of

MASTER OF SCIENCE IN MECHANICAL ENGINEERING

from the

NAVAL POSTGRADUATE SCHOOL
June 1971

ABSTRACT

This analysis is concerned with the use of radio-frequency (rf) current in producing lesions in the brain. The technique consists of passing the current between an active electrode implanted in the brain and an indifferent electrode located on the skull. The resistivity of the tissue causes electrical energy to be converted into heat thus raising the tissue temperature. A problem that is sometimes encountered is uncontrollable boiling of the tissue near the probe tip. A theoretical model which considers the combined effects of conduction, blood flow, metabolism, and rf heating is presented to show the relative effects of each of the terms on the temperature field. It was found that conductive effects and rf heating effects are very important parameters in predicting lesion size, while the blood flow effect is only marginally important. It is proposed that by maintaining the temperature of the probe at a low constant value, the maximum temperature of the lesion can be kept well below the boiling point, yet because currents and time can be increased, the volume of tissue destroyed equals or even surpasses that of the conventional probe. Finally, the radio-frequency probes are compared to resistively heated probes. The lesions produced by these probes are shown to be significantly smaller than the lesions produced by the rf probes.

TABLE OF CONTENTS

LIST OF TABLES

LIST OF ILLUSTRATIONS

NOTATION

Symbol	Description	Typical Units
α	Tissue thermal diffusivity	cm^2/sec
c_b	Blood specific heat	cal/(gm°C)
c	Tissue specific heat	cal/(gm°C)
C	Tissue capacitance	Farads
ε	Tissue dielectric constant	F/cm
I	Current	amps
k	Tissue thermal conductivity	cal/(cm°C sec)
l	Uninsulated length of probe	cm
m_b	Volumetric blood flowrate	$gm/(cm^3 sec)$
r	Radial location in tissue	cm
r_0	Probe radius	cm
R	Tissue resistance	ohm
S_m	Metabolic heat generation rate	$cal/(cm^3 sec)$
t	Time	sec
T	Tissue temperature	°C
T_b	Blood temperature	°C
T_0	Initial tissue temperature	°C
T_w	Tissue temperature at probe	°C
ω	Frequency of current	cycles/sec
Z	Impedance of tissue	ohm
ρ	Tissue density	gm/cm^3
ρ'	Tissue resistivity	ohm-cm

Non-dimensional Groups

$$R = \frac{r}{r_0} \qquad \beta = \frac{m_b c_b r_0^2}{k} \qquad \tau = \frac{\alpha t}{r_0^2} \qquad \phi = \frac{\theta}{G}$$

$$\theta = \frac{T - T_0}{T_0} \qquad G = \frac{I^2 \rho'}{16\pi^2 r_0^2 k T_0} \qquad G' = \frac{I^2 \rho'}{4\pi^2 l^2 k T_0} \qquad \theta_0 = \frac{T_w - T_0}{T_0}$$

ACKNOWLEDGEMENTS

I wish to express my sincere appreciation to my advisor, Professor Thomas E. Cooper, for his invaluable assistance during the past year. Under his capable guidance this thesis became an enjoyable experience as well as an interesting, rewarding challenge.

I would also like to express a very special thanks to a very special person, my beautiful wife, Karen. Her loving admiration and persevering faith proved to be a great source of encouragement and strength. I dedicate this thesis to you, Karen.

I. INTRODUCTION

A. STATEMENT OF PROBLEM

In order to treat certain disorders occurring in the central nervous system such as Parkinsonism, unbearable pain, and malignant tumors, surgeons at times find it necessary to surgically destroy discrete regions of nervous tissue. Numerous methods have been used by clinicians to accomplish tissue destruction. One such method, which has met with considerable success, employs a long, thin, needle-like probe which can be made to emit a low-power, continuous wave radio-frequency current. The probe itself serves as the emitting electrode and a second, indifferent electrode connected to some remote, external point on the body acts as a ground. As current is passed between the electrodes, the resistivity of the tissue causes electrical energy to be converted to tissue internal energy thus giving rise to an increase in local tissue temperature. A lesion, or region of destroyed tissue, is formed when the local tissue temperature is raised above approximately 55°C [3].

The major drawback of the radio-frequency probe has been excessive heating of the tissue in the immediate vicinity of the active electrode resulting in gas formation, carbonization of the tissue and adherence of the coagulum to the electrode. Gas formation is many times accompanied by minor "explosions" so that the method often reduces to a crude, brutal form of mechanical tissue destruction [35].

In order to aid surgeons in predicting and creating well controlled lesions, it is necessary to model the heat transfer process occurring in the region surrounding the active electrode. Several attempts have previously been made at formulating such a model [3, 35]; however, solutions which consider the combined interaction of tissue conductive effects, blood flow effects, metabolic effects, and radio-frequency heating effects on the change of tissue temperature with time have not yet been put forth. Such a model is presented in this thesis for spherical and cylindrical probes. The resulting equations are solved using a finite difference technique and presented in a form that can be readily used by surgeons.

As a proposed method of preventing excessive heating of the tissue, a constant temperature radio-frequency probe and a high resistance heating probe are also analyzed and discussed.

An additional objective is to present a summary of the various techniques that are used to create lesions in tissue. These techniques may be broken into several broad categories: mechanical, chemical, ultrasonic, radio-active, x-ray, freezing and electrical methods of destruction. A description of these methods, complete with the advantages and disadvantages of each, follows.

B. METHODS OF PRODUCING LESIONS

1. Mechanical Destruction

Perhaps the most conventional and familiar surgical technique is that in which the surgeon, through use of a scapel, manually makes an incision and removes or destroys unwanted tissue. This technique has been refined for use in the brain. A wire-like knife with a curved or angulated tip is concealed in a suitable length of hypodermic needle tubing of approximately 1½ mm. diameter. The needle is inserted in the brain to the required depth, and the knife is pushed out and rotated 360°, thus producing a lesion in the form of a body of revolution. Glees and others [17] have used this technique and note that the lesions produced are well localized but many times are large, irregularly shaped and lack uniformity. In addition, Carpenter and Whittier, [6] report that "The lesions appeared to be dependent upon interruption of local vascular patterns and to a variable extent upon the blood elements liberated into the tissue." As a result of this dependence, the "rotating knife" method has not proven successful in producing consistent, uniform lesions.

More obvious disadvantages of this mechanical method include profuse hemorrhaging, incidental tissue destruction, and infection.

2. Chemical Destruction

Localized necrosis (tissue destruction) is produced chemically by injecting a few drops of zinc chloride, chromic

acid, or similar corrosive chemical locally into the brain. The chemical tends to diffuse rapidly and large, irregularly shaped areas of tissue destruction are produced. Hyper-excitability, convulsions, and unusual pain are reported to follow lesions produced by this method. In addition, injected solutions tend to "leak" out around the needle and cause enlarged needle tracts and occasional cortical injury [6].

Because of the unpredictability of the size, shape and histological characteristics of the lesions produced by corrosive chemicals, this method is of little value for use in the brain.

3. Ultrasonic Destruction

Ultrasonic waves are mechanical vibrations in solid, liquid or gaseous mediums lying above the range of human hearing. The piezo-electric effect is adapted to the generation of ultrasonic waves at frequencies above 500 kilocycles (kc), the range most often used in biological work. Tissue is destroyed primarily by microscopic mechanical motion although heating is also present. Wood and Loomis [38] give an account of the effects of high frequency sound waves upon living matter.

The ultrasonic waves are produced by a quartz plate vibrating in resonance with a high-frequency current passing through the plate. It is possible to focus these waves at a central focal point by using a concave quartz plate. One can then concentrate as much as 150 times as

much ultrasonic energy at the focal point as is found in a region near the vibrating plate [20]. As a result, maximum tissue destruction occurs at the focal point while the intervening tissue remains relatively undamaged.

Experiments by Lynn and others [20] show that the ultrasonic technique causes an area of destruction on the scalp, followed by a region of normal, undamaged tissue, and finally a well defined focal point of severe destruction. They also found that once a lesion is initiated, it appears to extend rapidly and progress to non-irradiated parts of the brain.

Presently, the successful use of the ultrasonic technique is hindered by the scalp injury. Methods are now being studied to eliminate this surface destruction.

4. Radioactive Destruction

By implanting a small glass radon seed containing approximately 1 millicurie (mc) into a region of nervous tissue in the brain, one can create a sharp, circumscribed area of destroyed tissue of approximately 4 mm in diameter. Information concerning radon dosage values for the production of appropriate neural lesions is included in a paper by Borison and Wang [4].

Stein and Peterson [33] report that the lesions produced by radon seeds are circular and discrete; however, they are variable in size and volume of tissue destroyed. They postulated that "The volumes of tissue destroyed were not proportional to total radiation (millicuries-hours),

probably because of differences in radiosensitivity of different parts of the brain."

Not enough data were taken to develop conclusions, but the experimental lesions produced were not lethal and did not result in physiologic disturbances. The lesions were also well localized and consistent in configuration and histologic characteristics. Perhaps the major drawback of this technique at present is a lack of radiosensitivity information for the various locations in the brain. A knowledge of this property is needed to effectively predict lesion size.

5. X-ray Destruction

By stereotaxically orienting multiple x-ray beams through the skull, it is theoretically possible to focus the intersection of the beams at a predetermined location in the brain. This will result in tissue destruction at the focal point in much the same manner as the previously discussed ultrasonic technique.

Carpenter and Whittier [6] point out "The use of x-ray in stereotaxic technique appears promising, but such elaborate equipment in neuroanatomic laboratories is rare." In order to use this method, a detailed study would have to be under-taken so that stereotaxic orientation by mere location on the skull could be accomplished.

The advantage of this technique would be that predictable and controlled lesions could be made in the brain without opening the skull. Presently, the therapeutic beams

available for this method produce excessive scatter, and beams small enough to be appropriate in an experimental animal are not of sufficient intensity. There are x-ray beams that would produce the necessary intensity without excessive scatter, but their use for stereotaxic purposes is unnecessarily elegant.

6. Cryosurgery

Cryosurgery has proven to be quite useful for various applications in the brain, especially for surgery complicated by bleeding or patient discomfort [15].

The cryoprobe is a hollow tube connected to a source of liquid nitrogen. The probe is insulated throughout except at its hemispherical tip. By controlling the flow-rate of liquid nitrogen, the tip can be cooled as low as -196°C, causing the tissue in the immediate vicinity of the tip to freeze and thus be destroyed. The cryosurgical technique is bloodless and patient discomfort is minimal. In addition, the surgeon can produce only temporary numbing or can destroy a region of tissue. By observing a patient's reactions to the numbing effect, the surgeon can ascertain whether or not the probe is in the proper location before lowering the temperature to the lethal level.

A description of the lesion formed as the tissue freezes is given by Cooper and Trezck [10, 12]. A method is also presented whereby the lesion size for a probe of arbitrary dimensions can be predicted. The rate at which the temperature field develops is also considered, and a cryosurgical atlas is proposed. Both steady state and transient

situations are analyzed in their work. Another heat transfer model of the cryoprobe is given by Rutkin and Barish [29].

Cooper, Gionino, and Terry [9] describe the effects which contribute to lesion formation by freezing: the slowing down of the blood flow, congested blood vessels, dehydration and the resulting concentration of electrolytes, crystallization and the consequent rupture of cellular membranes.

Lack of hemorrhaging during the operation is a marked advantage of cryogenic surgery. The small amount of hemorrhaging that does occur is due to the mechanical passage of the probe through the brain tissue. However, one disadvantage of the cryosurgical technique is the relatively large probe size (2 mm. or greater).

7. Direct Current (dc)

It is possible to produce generally well localized lesions in the brain by applying a direct current between two electrodes: an active electrode inserted into the proper location in the brain, and an inactive electrode, or ground, placed on some other position in the body. The resistivity of the brain tissue causes electrical energy to be converted to heat, thus causing the local tissue temperature to be raised. When the tissue temperature is raised above 55°C, the tissue is destroyed.

This technique can be used with the active electrode serving as either a cathode or anode. When the electrode

acts as a cathode, the lesions formed are large and irregular due to the amount of gas formed at the tip [6]. In addition, Mullan and others [22] found the cathodal lesions to be hemorrhagic and hard to reproduce. Similarly the anodal lesions were also found to be irregular at higher currents. According to Mullan's work, using the electrode as an anode, surgeons can produce small and discrete lesions provided they slowly increase the current up to a maximum of 2 milliamps (ma) or prolong the duration of heating up to thirty minutes.

In general, however, lesions produced by the direct current method vary in size, shape and uniformity. Watkins [37] confirms the irregularity of the d-c lesions and adds that the lesions are too small for use in operations on man. He also states that "D-c devices suffer from an electrode polarization and have an additional disadvantage that the make-transients and break-transients stimulate muscle and nervous tissue." The polarization of the electrode is an uncontrolled variable of electrolysis and, along with the amount of gas formed at the electrode tip, is a cause for the lack of control over the extent of tissue destruction.

The fact that direct current stimulates the nerves is an advantage in one respect: the surgeon can be assured that the active electrode is in the proper location in the brain by observing a patient's reactions to the stimulating effect of the direct current.

The disadvantage of the nerve stimulation is more obvious. Other nerves, as well as those directly in the

lesion, could be stimulated during an actual operation. Furthermore, should the current find its way to the heart, it would cause the heart to quiver instead of pump. In effect, the surgeon would have created an electric chair effect.

An additional disadvantage of the dc method is that direct current tends to have preferred paths in the brain (paths of least resistivity) resulting in oval shaped lesions being produced.

One final disadvantage of the direct current method is noted by Herrero [18]: "Animals with dc lesions usually had extensive scar tissue present both around and infiltrated within the tissue." This scar tissue implies that the blood vessels along with the nervous tissue has been destroyed. Had the blood vessels remained, the body would more easily accommodate the lesion.

One of the advantages of the dc method over most of the methods discussed previously is that the small electrode can be painlessly inserted and causes minimal damage to the surrounding tissue while being inserted and retracted. In addition, hemorrhaging is not a significant problem with the dc method.

8. Radio-Frequency (rf) Current

The radio-frequency technique produces lesions in much the same manner as the direct current method. An active, needle-like electrode is inserted into the proper location in the brain, and an inactive electrode is placed on

the skull or some other remote portion of the body to serve as a ground. A low-power, continuous wave, radio-frequency current is passed between the electrodes. Tissue destruction is accomplished by resistive heating of the tissue itself. If the tissue temperature is raised above 55°C, the tissue is destroyed. The factors governing the amount of heat produced are the resistivity of the tissue, the size of the electrode, the amount of current used, and the length of time the current is applied. An inverse relation between current and time gives rise to the amount of energy. If not enough current is used, no tissue destruction occurs for an infinite amount of time. If too much current is used, violent boiling occurs immediately upon switching on the current.

Petty and others [26] conducted a study correlating tissue destruction with the frequency of the alternating current. They observed that low frequency current resulted in sporadic or no tissue destruction at all. If over 160 ma were applied at four (4) kilohertz (khz), sparks emanated from the electrode. As the frequency is increased above 45-khz and into the radio-frequency range, tissue destruction proceeds readily. Rowland, *et. al.* [28] offer an explanation for the lack of coagulation at low frequencies. They suggest that coagulation is dependent on the amount of charge per pulse. A unit of charge is a millicoulomb (mcoul.) and is equivalent to a milliamp (ma) times a second. The total energy applied by an alternating current is determined

by the number of mcoul. per pulse times the frequency of pulses per second times the length of time current is applied. Recall that the size of the lesion is dependent only on the current (mcoul. per pulse times frequency) and the time. Therefore, a low frequency current applied in a given amount of time has a greater charge per pulse (mcoul. per pulse) than does an equal amount of high frequency current in the same amount of time. This greater charge per pulse could possibly be what causes the sparks to emanate from the electrode.

In reference to the radio-frequency technique, Aronow [3] explains that "For surgical purposes it is necessary to have: (a) precise control of the size of the small volume of destruction; (b) precise control of the physical position of the lesion in a relatively inaccessible location; and (c) precise control of the functional position of the lesion."

There are many different set-ups of the radio-frequency apparatus presented in the literature [1, 3, 13, 14, 26, 31, 32, 34, 35, 36, 37]. Each of these set-ups contain certain advantages and disadvantages.

Excessive heating of the tissue immediately surrounding the electrode results with the apparatus proposed by Aronow [3]. The temperature exceeds 100°C and the tissue begins to boil as a result. In addition, there is gas formation, carbonization of the tissues and adherence of coagulum to the electrode. As the hard coagulum becomes encrusted

on the electrode, the total diameter of the electrode is increased and much damage to the surrounding brain tissue results as the probe is withdrawn from the brain. The gas formations are actually minor "explosions" so that the method reduces to a rather brutal mechanical method. Steam bubbles are formed around the tip of the electrode and block the path of the current. An audible popping sound is an indication to the surgeon that boiling is taking place. In addition to the obvious disadvantages that occur with boiling, it was noted that patients in which boiling occurred often become "somnolent and confused" [35].

In an attempt to prevent boiling from occurring, Van den Berg and Van Manen [35] designed their "Coagrader" which permits controlled and predictable lesions to be formed "within safe limits for physiological and clinical applications." In addition to controlling and predicting the size of the lesion, the surgeon must be certain of the physical location of the active electrode before irreversible damage is initiated. As a means of assuring proper probe location, low-frequency alternating current is passed between the electrodes and the patient's response is analyzed. Sias and Goodman [31] point out that low-frequency alternating current has the same stimulating effect as does direct current, whereas radio-frequency current has no stimulatory effect at all.

Another means in which a surgeon can check the probe location is discussed by Brodkey, *et. al.* [5]. They discovered

that a temperature range of 40-49°C can reversibly block nervous function. After positioning the electrode stereotaxically and raising the temperature of the tissue surrounding the electrode to the reversible range, a patient's response will indicate whether or not the probe is directly on target. The range of temperature in which reversibility occurs is a narrow one, however. In addition, measurement of the temperature of the tissue surrounding the electrode is not a simple task. It is easy enough to find the temperature of the probe tip by means of a thermal measuring device, but the tip temperature is not necessarily the true tissue temperature surrounding it. It was shown by Dieckmann and others [13] that during the first few moments of heating, the rate of increase in temperature is greater at a short distance away from the tip than at the tip itself due to conductive heat losses to the probe. Even externally applied thermocouples have been reported to distort the temperature field of the tissue [5]. It has been shown, however, that the radio-frequency technique has the fine control necessary to successfully heat reversibly [5].

One problem that has been evident with the r-f equipment concerns a defect in probe insulation. Large, irregularly shaped lesions have been known to form at points along the electrode tract due to current "leaks." Szekely and others [34] developed a stylet probe to minimize this "leak."

As with the dc probe, the very small size of the rf probe insures that the overlying brain tissue remains undamaged.

If the probe is introduced slowly, vascular structures can be pushed aside instead of punctured. Closure rapidly takes place as the probe is withdrawn, and discomfort to the patient is minimal [39].

After the probe is inserted in the brain, and the location of the probe has been checked, appropriate control of the physical parameters of time, tip exposure, and temperature allow well-circumscribed, reproducible lesions to be made [36]. The tip diameter also affects the size of the lesion produced.

The actual stages of coagulation are discussed by Petty and Edsall [26]. There are three stages of coagulation: (1) coalescense around the electrode; (2) uniform expansion in all directions (fast at first and then more slowly as the lesion progresses); and (3) boiling.

Note that, unlike the dc lesion, the rf lesion does not follow preferred paths in the brain but rather uniformity in all directions resulting in a well-circumscribed spherical lesion. The lesion contains three zones: a central core of dense dead tissue surrounded by a zone of damaged tissue and finally, a narrow zone of granulations which clearly mark the border of the lesion [2].

Mark, *et. al.* [21] point out that the blood vessels running through a lesion are often times spared. "This is partially true when the temperatures used at the tip are below 80°C." Heating above 100°C results in rupturing the blood vessels. As was noted earlier, this corresponds to the boiling temperature.

In summary, the radio-frequency method allows controlled and predictable spherical lesions to be produced within safe limits for physiological and clinical applications. Hemorrhaging is not a problem and discomfort to the patient is minimal. There are two methods available with which to check the probe location before irreversible destruction of the tissue begins. The system has precise control over the volume of destruction and often times the blood vessels running through the lesion can be spared. Boiling tends to be a problem with this technique, but proper control of various physical parameters can avoid boiling.

II. PHYSICAL ANALYSIS

A region of nervous tissue in the brain is quite complex. It contains blood vessels, ventricles and is nonuniform in composition. The grey matter in the brain seems to have a higher resistance to temperature than does the white matter [13]. Although the thermal properties (heat capacity, thermal conductivity, density and thermal diffusivity) are known to within an accuracy of 5% [11], there are still many variables in the brain whose exact values and temperature coefficients are uncertain, i.e., specific resistance, dielectric constant and circulation.

Realizing these difficulties, a simplified, one dimensional heat transfer model of the radio-frequency probe will now be developed. Consider the brain to be an infinite, homogeneous, imperfect dielectric of resistivity ρ' and dielectric constant ε. The active electrode is considered to be a conductive sphere of radius r_0 embedded in the brain, while the indifferent electrode is a spherical conductor surrounding the brain (see Figure 1).

The impedance of a spherical shell of material of width Δr can be represented by an incremental capacitance dC in parallel with an incremental resistance dR [35] (see Figure 2):

$$dC = \varepsilon \cdot \frac{4\pi r^2}{\Delta r} \quad ; \qquad dR = \rho' \frac{\Delta r}{4\pi r^2} \quad ;$$

$$dZ = \frac{dR}{1 + j\omega dR dC} = \frac{dR}{1 + j\omega\rho'\varepsilon} \quad .$$

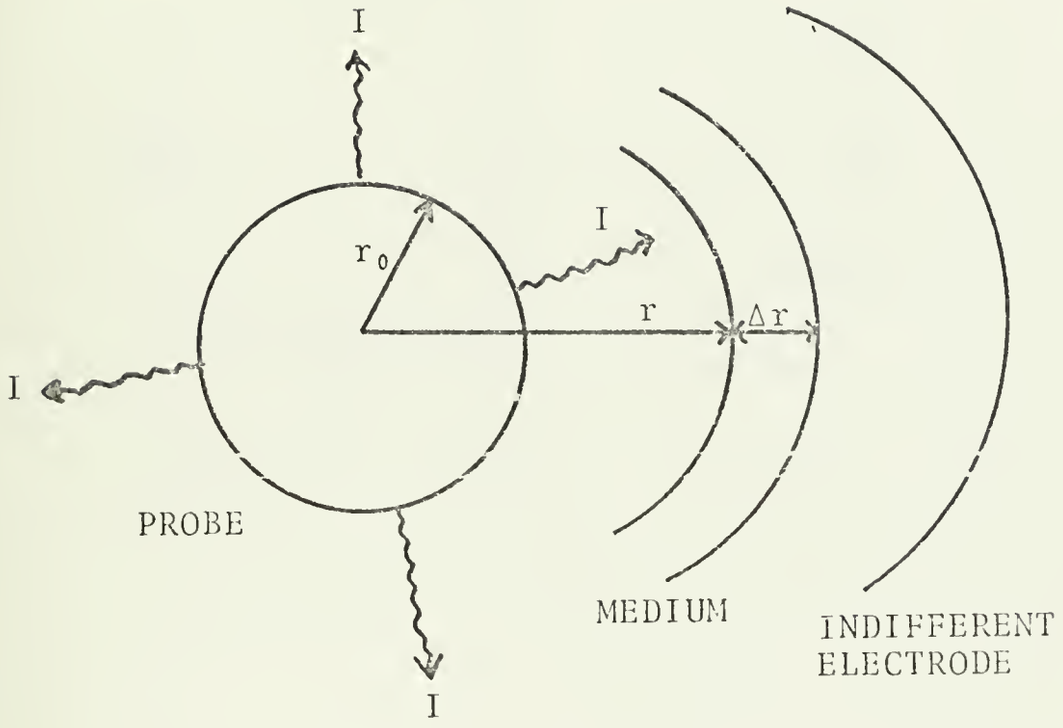

Figure 1. Model of Spherical Probe.

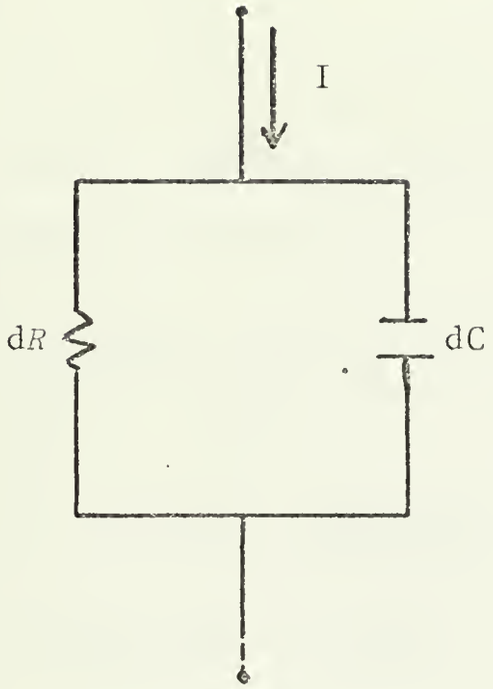

$$dC = \varepsilon \cdot \frac{4\pi r^2}{\Delta r}$$

$$dR = \rho' \frac{\Delta r}{4\pi r^2}$$

$$dZ = \frac{dR}{1+j\omega dR dC}$$

Figure 2. Impedance of the System.

The total impedance of the system can be obtained by integrating dZ [35]:

$$Z = \int_{r_0}^{\infty} dZ = \frac{1}{1+j\omega\rho'\varepsilon} \int_{r_0}^{\infty} dR = \frac{1}{1+j\omega\rho'\varepsilon} \left[\frac{\rho'}{4\pi r_0}\right].$$

At radio-frequencies, however, $|j\omega\rho'\varepsilon| \ll 1$ for brain tissue [3, 35] and the impedance reduces to $Z = \rho'/4\pi r_0$. For example, for brain tissue:

$\rho' \simeq 150\text{-}200$ ohm-cm [35]

$\varepsilon \simeq 70\ \varepsilon_0$ [35]

$$\varepsilon_0 \simeq 8.85\times10^{-12}\ \frac{\text{coulomb}^2}{\text{newton-m}^2} = 8.85\times10^{-14}\ \frac{\text{sec}}{\text{ohm-cm}}$$

$$\varepsilon = 6.195\times10^{-12}\ \frac{\text{sec}}{\text{ohm-cm}}$$

Take

$\rho' = 200$ ohm-cm

then

$\rho'\varepsilon = 12\times10^{-10}$ sec.

Hence,

$|j\omega\rho'\varepsilon| = 12\times10^{-10}\ \omega$

where

ω is in Hz.

Radio-frequencies range from 10 kHz to above the megahertz (MHz) frequency. Clearly, even in the megahertz range, $|j\omega\rho'\varepsilon| \ll 1$, i.e. for 10MHz:

$$\omega = 10\times10^{6}\ \text{Hz}$$

$$\therefore\ |j\omega\rho'\varepsilon| = 12\times10^{-3} \ll 1.$$

As a result, in the radio-frequency range virtually all of the current passes through the resistive leg of the circuit shown in Figure 2.

To solve for the temperature field emanating from the radio-frequency probe, a one-dimensional energy balance is applied to a spherical element of tissue (see Figure 3):

> Heat into element by conduction - Heat out of element by conduction + Heat generation due to metabolism + Heat input due to blood flow + Heat generation due to rf heating = Increase in internal energy of element. (1)

Equation (1) can be reduced by substituting the following terms:

(i) Cross-sectional area = $A = 4\pi r^2$

(ii) Elemental volume = $\Delta V = 4\pi r^2 \Delta r$

(iii) Heat in by conduction = $q_{in} = -kA \frac{\partial T}{\partial r} = -4\pi r^2 k \frac{\partial T}{\partial r}$

(iv) Heat out by conduction = $q_{in} + \frac{\partial q_{in}}{\partial r} + \frac{1}{2!} \frac{\partial^2 q_{in}}{\partial r^2} \Delta r^2 + \cdots$

(Taylor Series)

(v) Heat generation due to metabolism =

$S_m \Delta V = S_m 4\pi r^2 \Delta r$

(vi) Heat addition due to blood flow =

$m_b c_b (T_b - T) \Delta V = m_b c_b (T_b - T) 4\pi r^2 \Delta r$

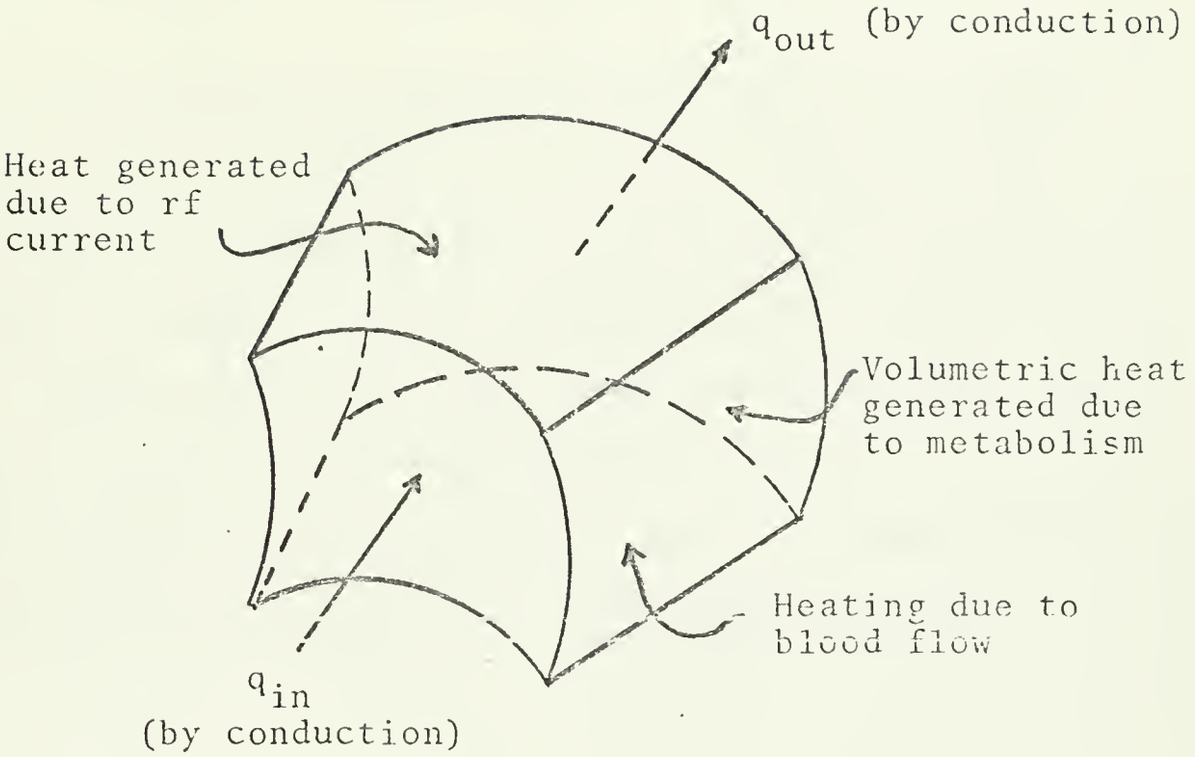

Figure 3. One-dimensional Energy Balance on Spherical Element.

(vii) Heat generation due to rf current =

$$I^2 dR = \frac{I^2 \rho' \Delta r}{4\pi r^2}$$

(viii) Increase in internal energy =

$$\rho c \frac{\partial T}{\partial t} \Delta V = \rho c \frac{\partial T}{\partial t} 4\pi r^2 \Delta r.$$

Note that in the model the effect of blood flow is treated as a perfect heat exchanger; that is, it is assumed that the blood acquires the tissue temperature as it exits a unit volume of tissue. This is consistent with a model first set forth by Perl [24, 25]. Rosomoff and Holaday [27] give values for the volumetric blood flowrate m_b.

If the metabolic heat generation rate is assumed to be a constant, it can be combined with the blood flow term as

$$m_b c_b (T_0 - T)$$

where

$$T_0 = T_b + \frac{S_m}{m_b c_b} .$$

This corresponds to redefining the reference temperature. It was shown by Cooper and Trezek [10] that in the case of brain tissue, T_0 is on the order of 0.5°C higher than the systemic arterial blood temperature T_b. For the case of a radio-frequency probe, the blood flow convects a portion of the heat generated in the tissue due to radio-frequency effects away from the probe tip.

Upon substituting (i-viii) into (1), the following equation results:

$$- \frac{\partial q_{in}}{\partial r} \Delta r + \frac{I^2 \rho' \Delta r}{4\pi r^2} + m_b c_b (T_0 - T)\ 4\pi r^2 \Delta r$$

$$= \rho c \frac{\partial T}{\partial t} 4\pi r^2 \Delta r + 0(\Delta r^2). \qquad (2)$$

Dividing (2) by Δr and taking the limit as $\Delta r \to 0$ yields

$$- \frac{\partial q_{in}}{\partial r} + \frac{I^2 \rho'}{4\pi r^2} + m_b c_b (T_0 - T)\ 4\pi r^2 = \rho c \frac{\partial T}{\partial t} 4\pi r^2. \qquad (3)$$

Note that

$$q_{in} = -4\pi r^2 k \frac{\partial T}{\partial r}.$$

Hence,

$$\frac{\partial \left\{4\pi r^2 k \frac{\partial T}{\partial r}\right\}}{\partial r} + \frac{I^2 \rho'}{4\pi r^2} + m_b c_b (T_0 - T) 4\pi r^2 = \rho c \frac{\partial T}{\partial t} 4\pi r^2. \qquad (4)$$

If k is assumed to be constant and (4) is divided by $4\pi r^2$, the equation becomes

$$\frac{k}{r^2} \frac{\partial \left(r^2 \frac{\partial T}{\partial r}\right)}{\partial r} + \frac{I^2 \rho'}{16\pi^2 r^4} + m_b c_b (T_0 - T) = \rho c \frac{\partial T}{\partial t}. \qquad (5)$$

It is now convenient to introduce the following non-dimensional variables:

$$R = \frac{r}{r_0} \text{ (Distance)} \qquad \beta = \frac{m_b c_b r_0^2}{k} \text{ (Blood Flow Term)}$$

$$\tau = \frac{\alpha t}{r_0^2} \text{ (Time)} \qquad G = \frac{I^2 \rho'}{16\pi^2 r_0^2 k T_0} \text{ (rf Heating Term)}$$

$$\theta = \frac{T - T_0}{T_0} \text{ (Temperature)} \qquad \phi = \frac{\theta}{G}$$

Substituting these variables into (5) yields

$$\frac{1}{R^2}\frac{\partial\left(R^2\frac{\partial\theta}{\partial R}\right)}{\partial R} - \beta\theta + \frac{G}{R^4} = \frac{\partial\theta}{\partial\tau} \qquad (6)$$

The boundary conditions are

(a) at the probe surface ($r=r_0$ or $R=1$) no heat is conducted from the brain tissue back into the probe, or

$$\left.\frac{\partial\theta}{\partial R}\right|_{R=1} = 0;$$

(b) at large distances from the probe the temperature of the tissue remains constant; that is, as $r\to\infty$, $T\to T_0$, or in non-dimensional form, as $R\to\infty$, $\theta\to 0$.

The initial condition is that at time $t=0$, $T=T_0$ or $\theta=0$ for all locations in the brain.

Equation (6) along with the boundary conditions and initial condition can be put in finite difference form and solved on the digital computer. For the details of this operation, the reader is referred to Appendix A.

A similar analysis can be carried out for a cylindrical probe resulting in the following equation:

$$\frac{1}{R}\frac{\partial\left(R\frac{\partial\theta}{\partial R}\right)}{\partial R} - \beta\theta + \frac{G'}{R^2} = \frac{\partial\theta}{\partial\tau}\ , \qquad (7)$$

where

$$G' = \frac{I^2\rho'}{4\pi^2 l^2 k T_0}\ ;\quad \theta,\ R,\ \text{and}\ \beta\ \text{are the same as above.}$$

The boundary conditions and the initial condition are the same as for the spherical probe. Equation (7) can also be solved by the finite difference scheme. The reader is referred to Appendix B for the details of the cylindrical solution.

Note that for both geometries the rf heating term dies off rapidly as the radius increases. This implies that the majority of the rf heating is generated close to the probe tip.

As was mentioned in the Introduction, a problem that exists with conventional rf probes is tissue boiling near the tip. If the tissue temperature is raised above approximately 100°C, the rf technique reduces to no more than a crude mechanical technique. It will be shown that even for moderate currents, unwanted boiling may occur. In order to prevent vaporization at the tip of the probe, it is proposed that a constant temperature probe be developed such that the maximum temperatures may be lowered and moved away from the probe tip. The solution to this problem is obtained in the same manner as for the "insulated" sphere except that one boundary condition is changed, namely the temperature at the probe tip is now treated as a constant. The results of this method are discussed in the next section.

Another technique used to destroy nervous tissue in the brain employs a "high-resistance" probe. In this method the current heats the probe tip rather than the tissue, resulting in heat diffusing through the tissue by conduction. This type of probe is discussed by Gildenberg [16]. One can solve for the temperature field by solving equation (6) with the rf heating term equal to zero and using the constant temperature boundary condition. Therefore, the equation to be solved is

$$\frac{1}{R^2}\frac{\partial\left(R^2\frac{\partial\theta}{\partial R}\right)}{\partial R} - \beta\theta = \frac{\partial\theta}{\partial\tau} \quad . \tag{8}$$

This equation can also be easily solved using the finite difference scheme. However, there is a closed form solution to this type of problem stated in Carslaw and Jaeger [7]. See Appendix C for details. This solution, when compared to the numerical solution, additionally serves as a check on the numerical scheme (Appendix C).

III. RESULTS AND DISCUSSION

In a previous attempt at modeling the radio-frequency probe, Aronow [3] assumed that "Distribution of heat normally takes place primarily by convection via the blood flow, rather than simple conduction." He then postulated a model that neglected blood flow and conduction entirely. It was assumed that all the heat generated due to rf current went into increasing the internal energy of the tissue. The simplified model did not correspond well to experimental data. Aronow indicated that neglecting conduction and blood flow are the most probable reasons for this lack of agreement.

Van Den Berg and Van Manen [35] have extended Aronow's model somewhat. They include the conduction term along with the radio-frequency term but neglect the blood flow term in establishing a steady state solution. They conclude that the blood flow effect is negligible and that the model is a good approximation of the true system. Experiments with egg white are in good agreement with their theoretical analysis.

As was seen in the Physical Analysis Section, the present model includes the combined effects of rf heating, blood flow, and conduction in analyzing the transient as well as the steady state solutions. Numerical results for both the spherical and cylindrical probe are given in Tables I-XVI. Values for θ/G are given at various non-dimensional locations (R) and times (τ) for various values of the blood flow parameter β (Tables I-VIII). Similarly, values for θ/θ_0 are given

for the constant temperature cylinder and sphere (Tables IX-XVI).

The relative effects of conduction, blood flow, time, and current will now be discussed. In addition, the constant temperature probe and the high-resistance probe will be compared to the insulated probe to show the relative advantages of each.

A. THE EFFECT OF CONDUCTION OF THE TEMPERATURE FIELD

Figures 4 and 5 are graphs of the non-dimensional temperature versus the radial location in the tissue for the blood flow parameter, β, equal to zero and non-dimensional time τ equal to ten (corresponds to a real time of approximately 2.5 seconds for a probe with a radius of 0.05 cm.). Two curves are presented: the dashed line represents Aronow's solution which neglects conduction, and the solid line represents a solution which includes conductive effects. Note that for a G of 1.0 (corresponds to applying a current of slightly greater than 2 ma for a 0.05 cm probe), θ is 10 at the spherical probe tip (R=1.0) if conduction is neglected (Aronow's assumption). This value is well in excess of the boiling temperature, i.e. boiling occurs at T≈100°C, the initial temperature of the tissue is approximately 37°C, therefore

$$\theta_{boiling} = \frac{T_{boiling} - T_0}{T_0} = \frac{100-37}{37} \simeq 1.7.$$

It is obvious from Figures 4 and 5 that conduction greatly reduces the temperature at the probe tip compared to what the

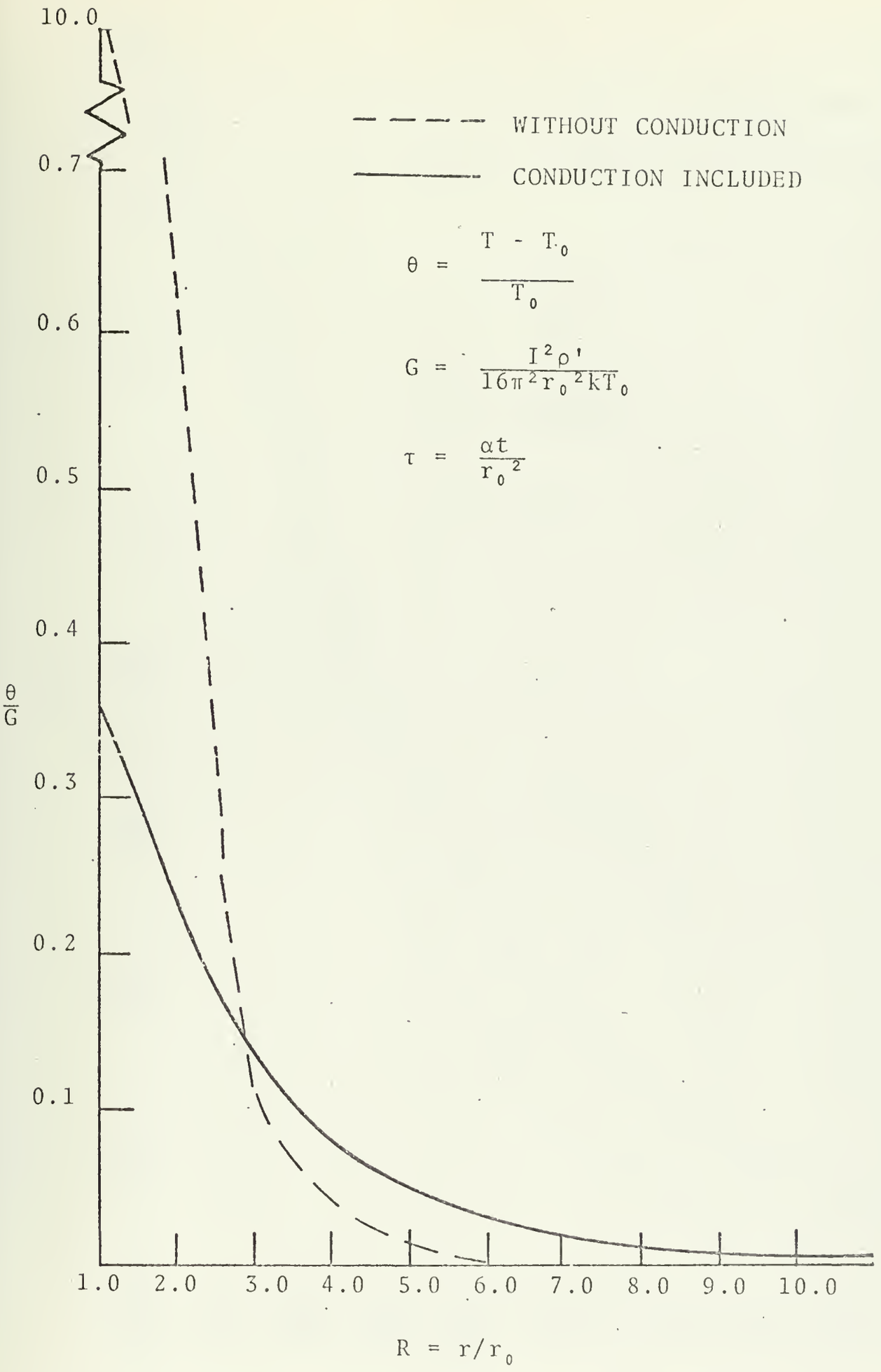

Figure 4. The Effect of Conduction on a Spherical Probe, $\beta = 0.0$, $\tau = 10.0$.

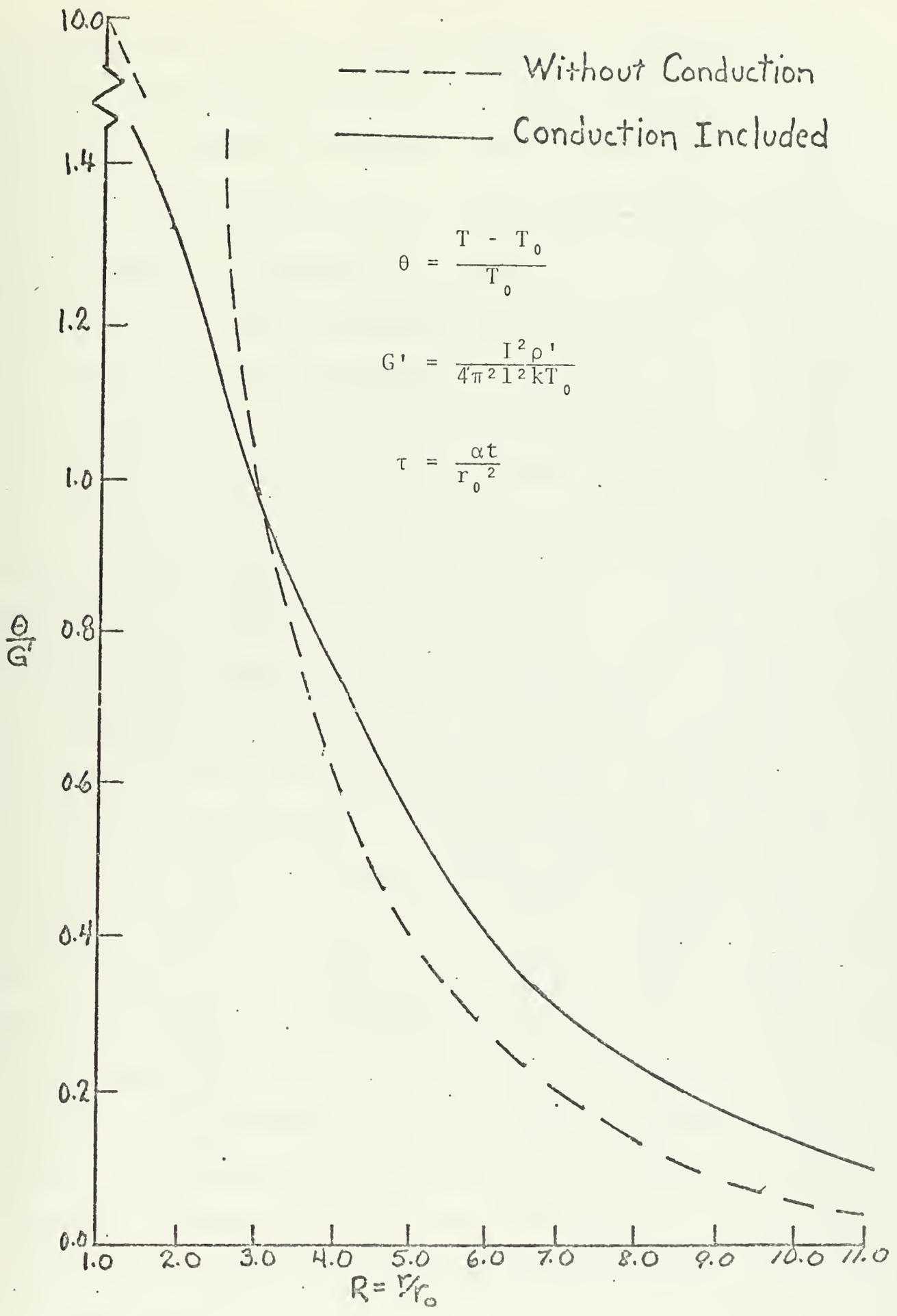

Figure 5. The Effect of Conduction on a Cylindrical Probe, $\beta = 0.0$, $\tau = 10.0$.

tip temperature would be in the absence of conduction. Hence, a significant portion of the heat generated near the probe tip is rapidly conducted away from the tip.

B. THE EFFECT OF BLOOD FLOW ON THE TEMPERATURE FIELD

Figure 6 is a graph of the temperature response in the brain due to a radio-frequency current emitted from a spherical probe at a non-dimensional time of ten. Both conductive effects and blood flow effects are included in this graph. Recall that all previous models assumed the blood flow effect to be negligible. Note from the graph that the cooling effect of blood flow decreases the temperature uniformly throughout the tissue. As the blood flow parameter, β, is increased, the temperature is lowered further. Because the blood passing through the lesion has a lower temperature than the heated tissue, heat is convected out of this region, thus reducing the temperature. To gain a feeling for the magnitude of this effect a typical value of β will be calculated. A typical value for $m_b c_b$ of blood-flow in the brain is 0.01 cal/cm^3/sec/°C [25] and a typical value of the thermal conductivity of brain tissue is 0.0014 cal/cm/°C/sec [11]. For brain tissue, therefore, β is approximately equal to $7\ r_0^2$, where r_0 is the probe radius expressed in centimeters. A typical radio-frequency probe might have a radius of 0.05 cm; therefore, β would be on the order of 0.02. As can be seen from Figure 6, this value for blood flow marginally decreases the temperature.

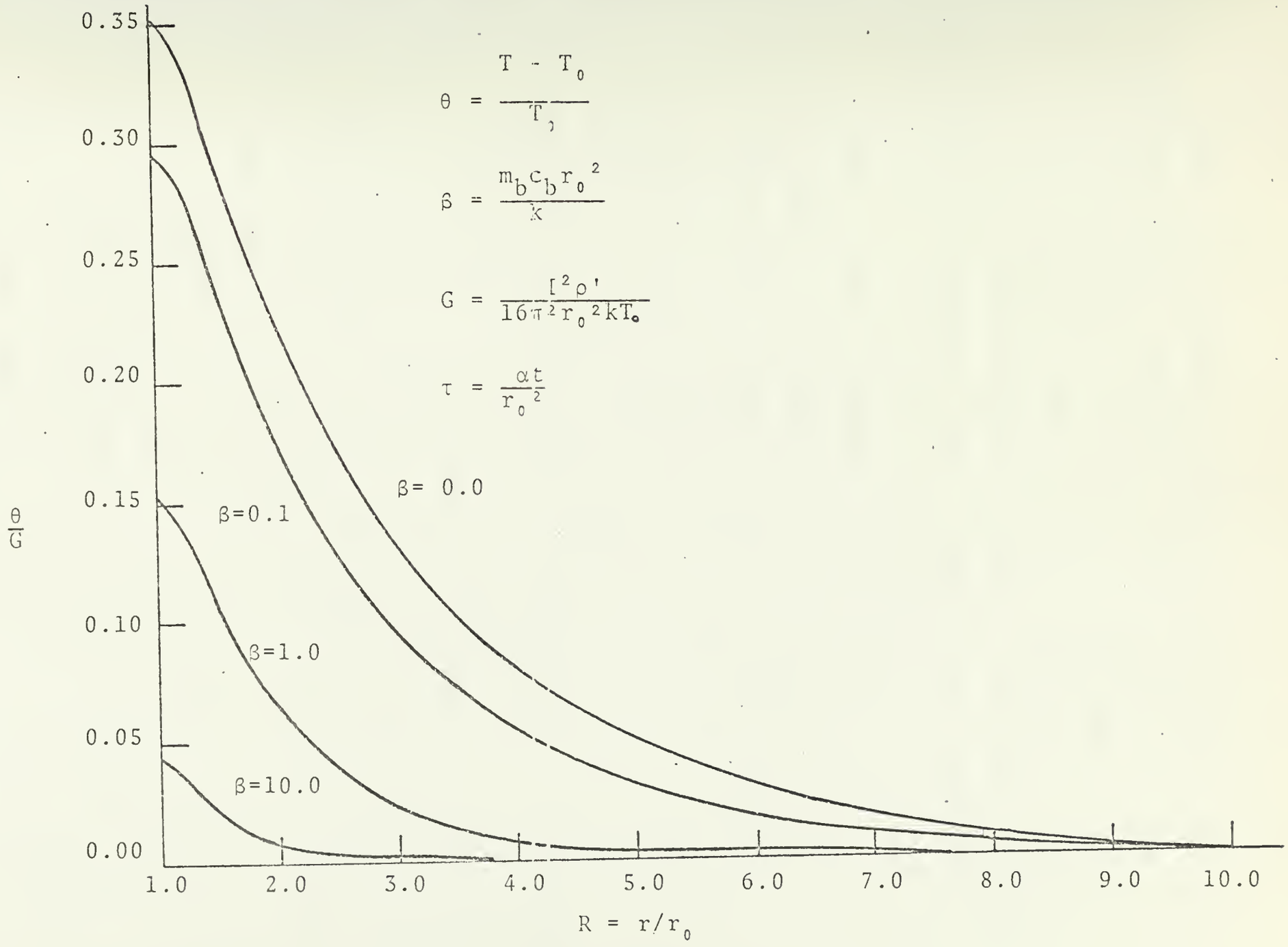

Figure 6. The Effect of the Blood Flow Parameter, β, on a Spherical Probe, τ = 10.0.

Figure 7 is a graph of the blood flow effect assuming a cylindrical probe. Blood flow is seen to play a slightly larger role in Figure 7 than Figure 6. The higher values for β depicted on the graphs serve to illustrate the trend that the blood flow parameter has on the lesion size. Again, the blood flow parameter tends to decrease the temperature in the lesion resulting in a slightly smaller lesion.

Figures 8 and 9 illustrate another effect of blood flow. In these figures the temperature at the probe tip (R=1.0) is plotted against time for the spherical and cylindrical probes. At low times the blood flow effect seems to be negligible, but as time is increased, the effect of blood flow becomes very noticeable. At τ equal to 10 it can be seen that the effect of blood flow is not negligible. For a probe of radius r_0 equal to 0.05 cm, τ of 10 corresponds to approximately 2.5 seconds. As the time is prolonged, the blood flow effect is increased even more. The larger values for β point out how increased blood flows cause steady state or equilibrium to occur at an earlier time. Again blood flow is shown to decrease the size of the lesion.

Since the probe radius enters the blood flow term as a squared term, one can see that as the probe radius is increased, the blood flow effects are sharply increased. For a larger probe the blood flow effect becomes a very important parameter. For the small probes and small times used in the rf technique, however, the blood flow effects are only marginally important.

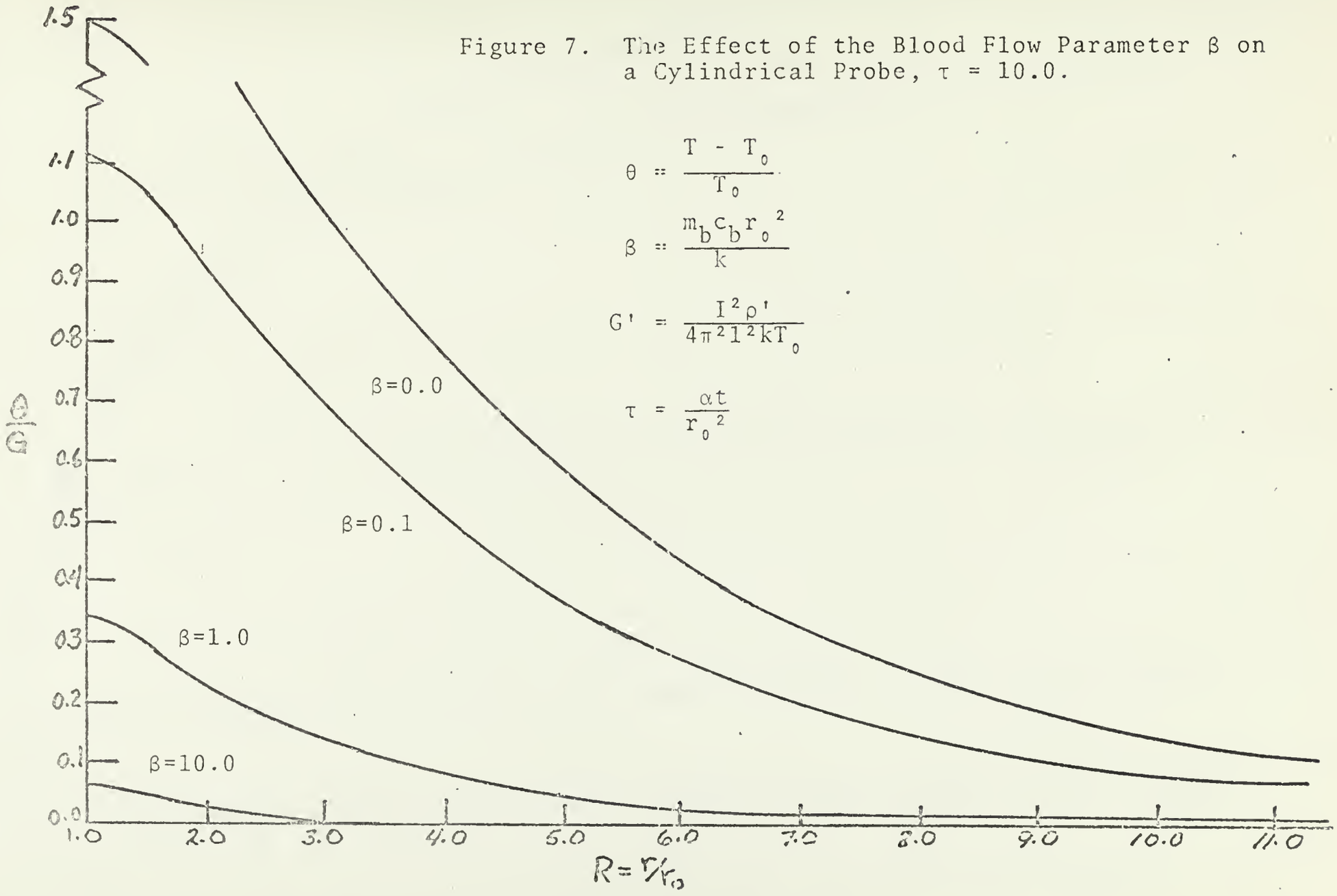

Figure 7. The Effect of the Blood Flow Parameter β on a Cylindrical Probe, $\tau = 10.0$.

$$\theta = \frac{T - T_0}{T_0}$$

$$\beta = \frac{m_b c_b r_0^2}{k}$$

$$G' = \frac{I^2 \rho'}{4\pi^2 l^2 k T_0}$$

$$\tau = \frac{\alpha t}{r_0^2}$$

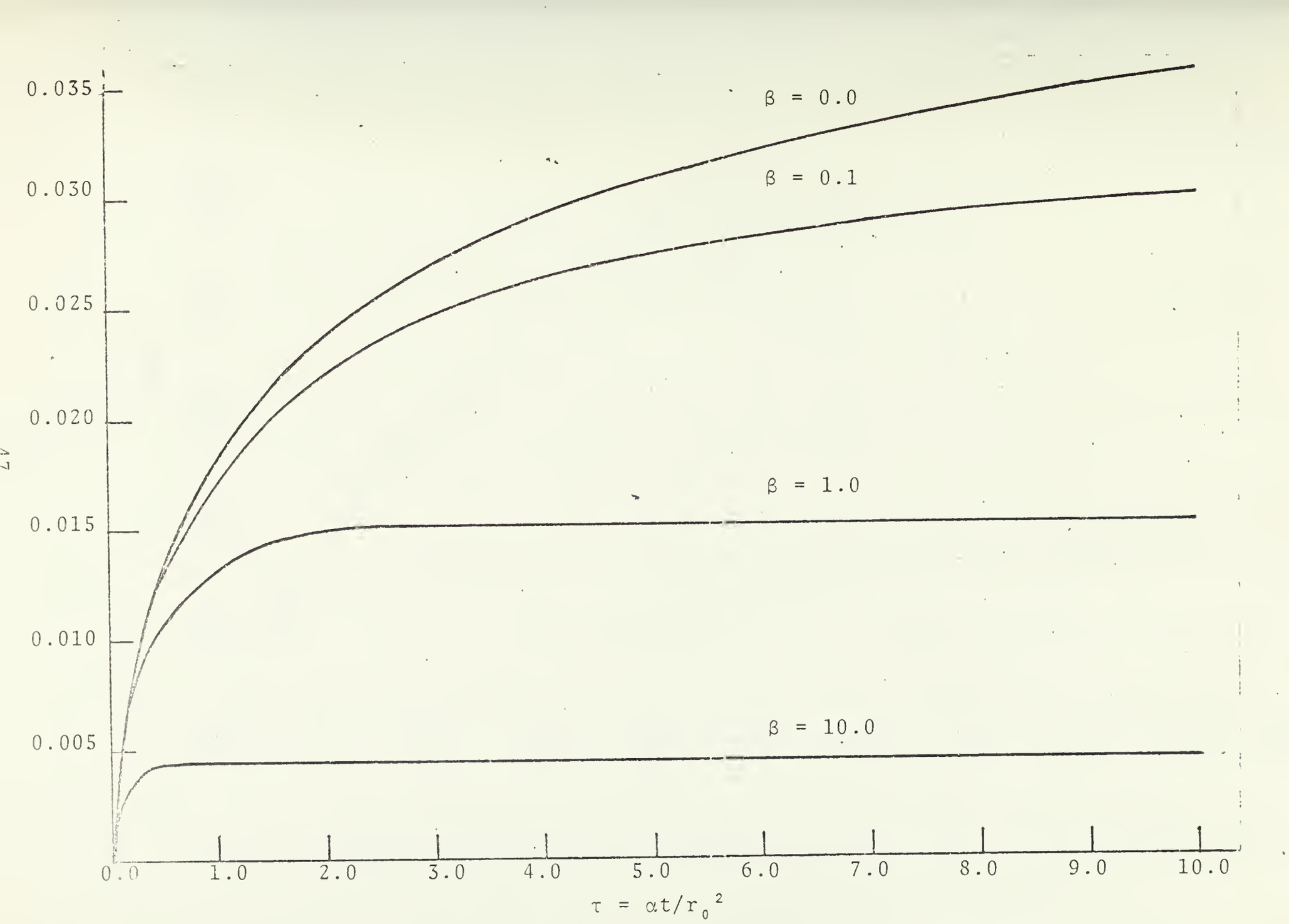

Figure 8. The Effect at the Probe Tip (R=1.0) of the Blood Flow Parameter, β, at Various Times (τ) for a Spherical Probe.

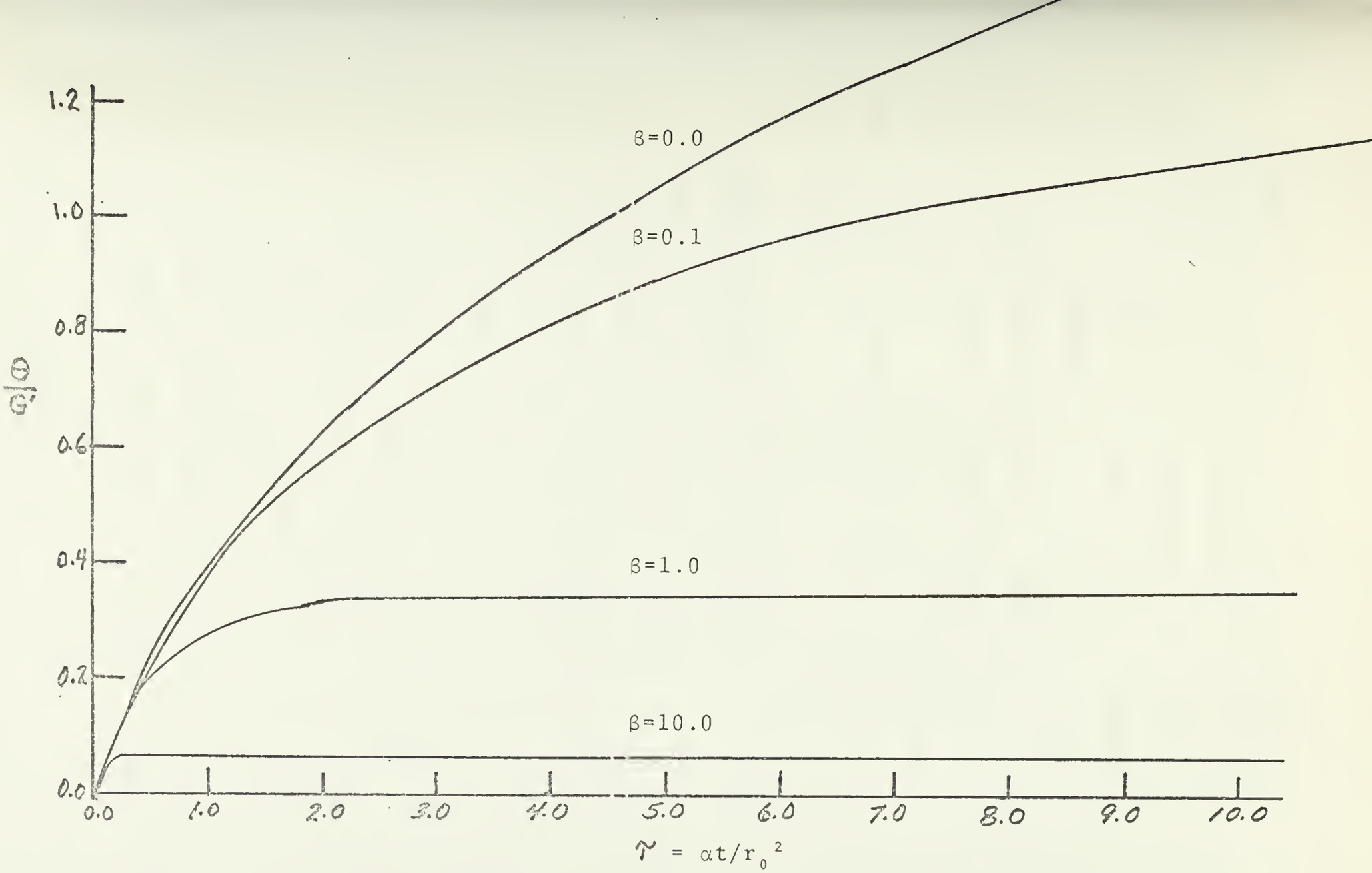

Figure 9. The Effect at the Probe Tip (R=1.0) of the Blood Flow Parameters β at Various Times (τ) for a Cylindrical Probe.

C. EFFECT OF INCREASED TIME ON TEMPERATURE FIELD

The previous section pointed out the fact that the effect of blood flow was increased as time was increased. Figure 10 indicates the trend of the rf temperature field as the time is increased. One can see that at small times, the rate of temperature increase is large, but as times increase, the rate of increase in temperature is lessened until steady state is reached. Steady state occurs at approximately τ equal to 130 (corresponds to about 36 seconds for a 0.05 cm probe radius).

D. EFFECT OF rf HEATING TERM ON TEMPERATURE FIELD FOR INSULATED PROBE

Figure 11 illustrates how the probe tip temperature is greatly increased as the rf current term is increased. Recall that a value of θ of 1.7 corresponds approximately to the boiling point. One can see that a G of 5 is close to this critical value for θ at the probe tip at time τ=10. If the resistivity of brain tissue is assumed to be about 150Ω cm [35], the thermal conductivity of the tissue is assumed to be 0.0014 cal/cm/°C/sec [11], the initial temperature of the tissue 37°C [3], and a probe of radius 0.05 cm, a G of 5 corresponds to a current of about 50 ma. In other words, if a current of 50 ma is applied for times longer than about 3 seconds, boiling will occur. In order to prevent boiling, a much lower current must be used, (about 30 ma).

E. CONSTANT TEMPERATURE PROBE

It is proposed that boiling can be avoided altogether if a constant temperature probe is used rather than an insulated

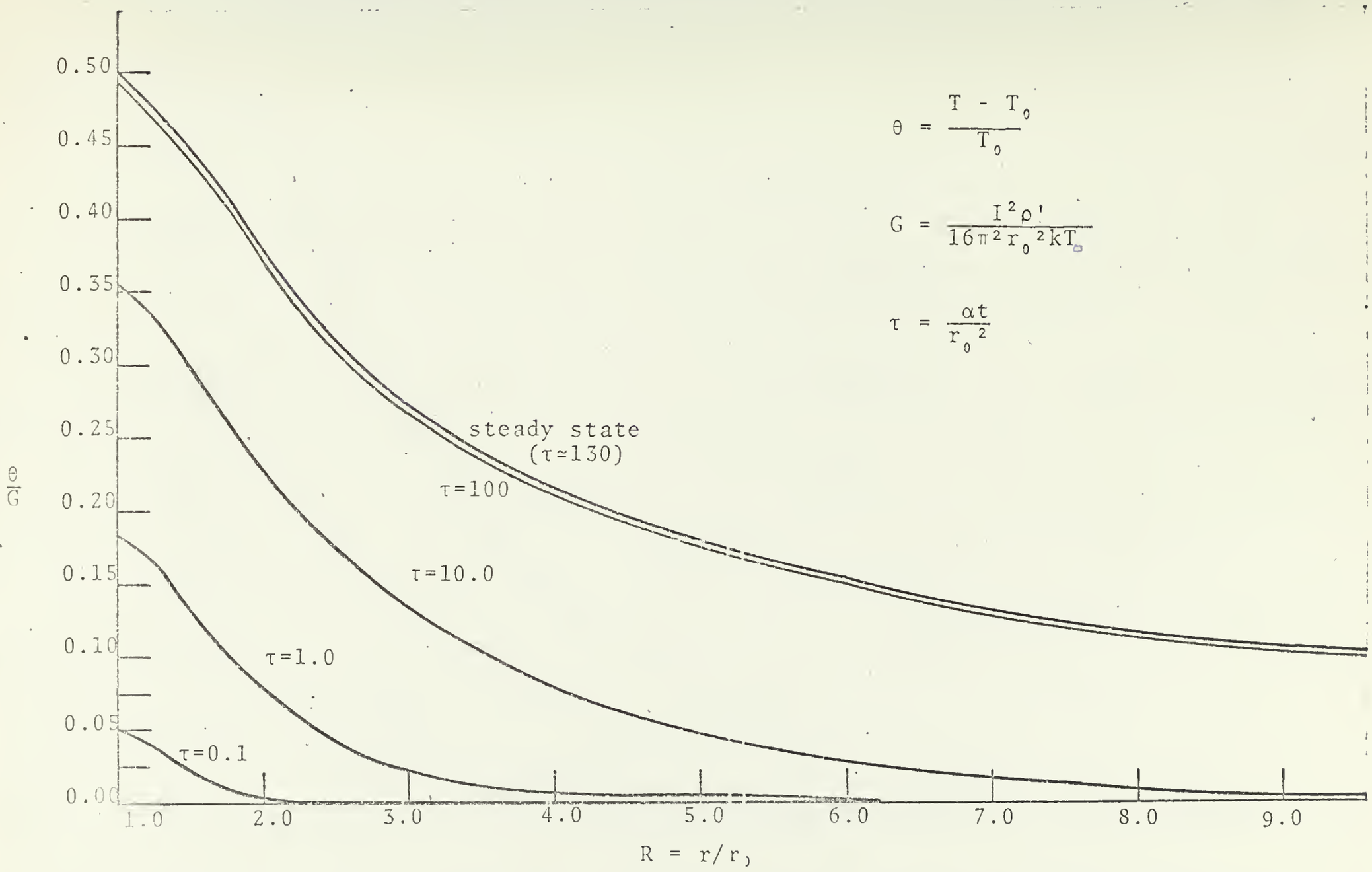

Figure 10. θ/G vs. R for Various Values of τ Assuming a Spherical Probe, β=0.0.

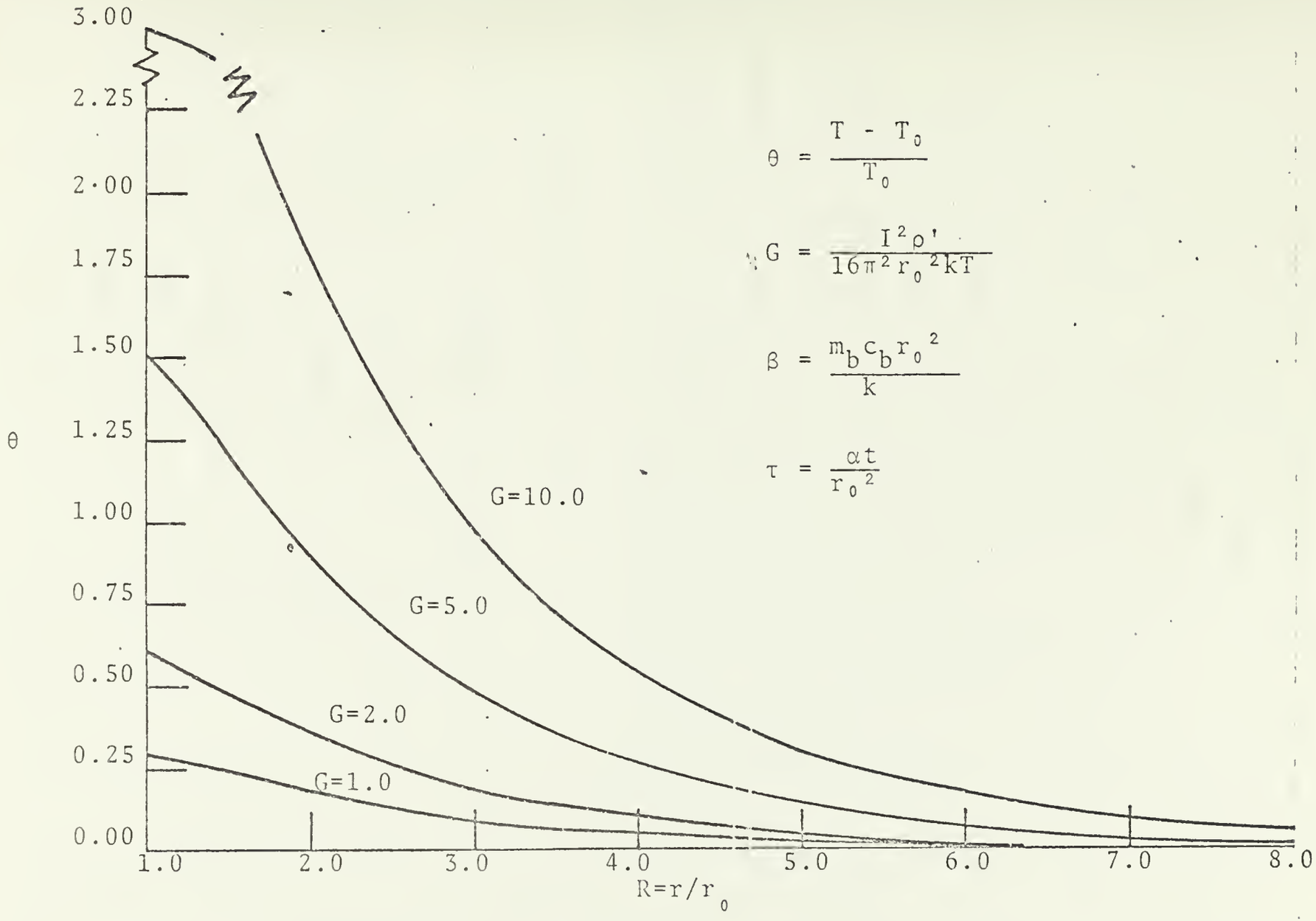

Figure 11. θ vs. R for Various Values of G for an Insulated Probe (Spherical) $\beta=0.1$, $\tau=10.0$.

probe. Figure 12 is a graph depicting the temperature profile in the brain for various values of the radio-frequency heating term G for a constant temperature spherical probe ($T \simeq 48°C$, $\beta = 0.1$, $\tau = 10.0$). As G is increased, the maximum temperature is moved away from the probe tip. The temperature profile is more flattened than it was with the insulated probe (see Figure 11). Note that the maximum temperature, even for a G as high as 10, is well below the boiling point ($\theta \simeq 1.7$), so there is a great margin of safety with this probe. Figure 13 gives a better indication of this safety factor. In this graph the insulated probe is compared to the constant temperature probe for a given value β, G, and τ. The insulated probe is close to the boiling point for τ of 10 whereas the constant temperature probe is well below the boiling point. The lesion radius depicted by the insulated probe for τ of 10 is approximately 0.16 cm, i.e.

$$T_{Lesion} \simeq 55°C, \; T_0 \simeq 37°C$$

$$\theta_{Lesion} = \frac{T_{Lesion} - T_0}{T_0} = \frac{55 - 37}{37} \simeq 0.49$$

From Figure 13, $\theta \simeq 0.49 \Longrightarrow R = r/r_0 \simeq 3.2$. For $r_0 = 0.05$ cm, r= 0.16 cm or the lesion extends (.16-.05) cm or 0.11 cm from the probe. For G=5.0, $\beta = 0.1$, and $\tau = 10$, the size of the lesion produced by the constant temperature probe is considerably smaller. However, the constant temperature probe is well below the boiling point, whereas the insulated probe is dangerously close. In addition, the current and time can easily

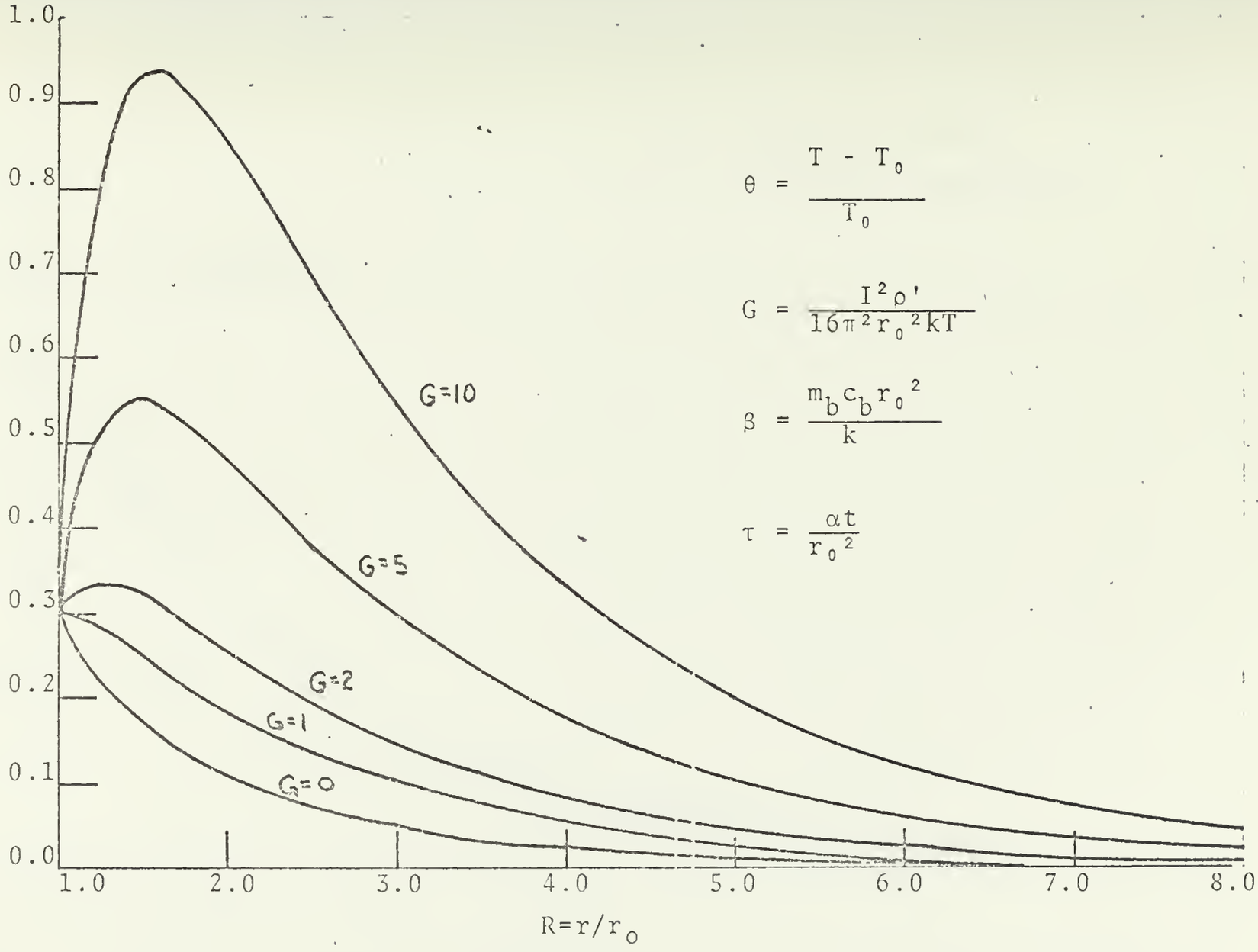

Figure 12. θ vs. R for Various Values of G for a Constant Temperature Spherical Probe, $\beta=0.1$, $\tau=10.0$.

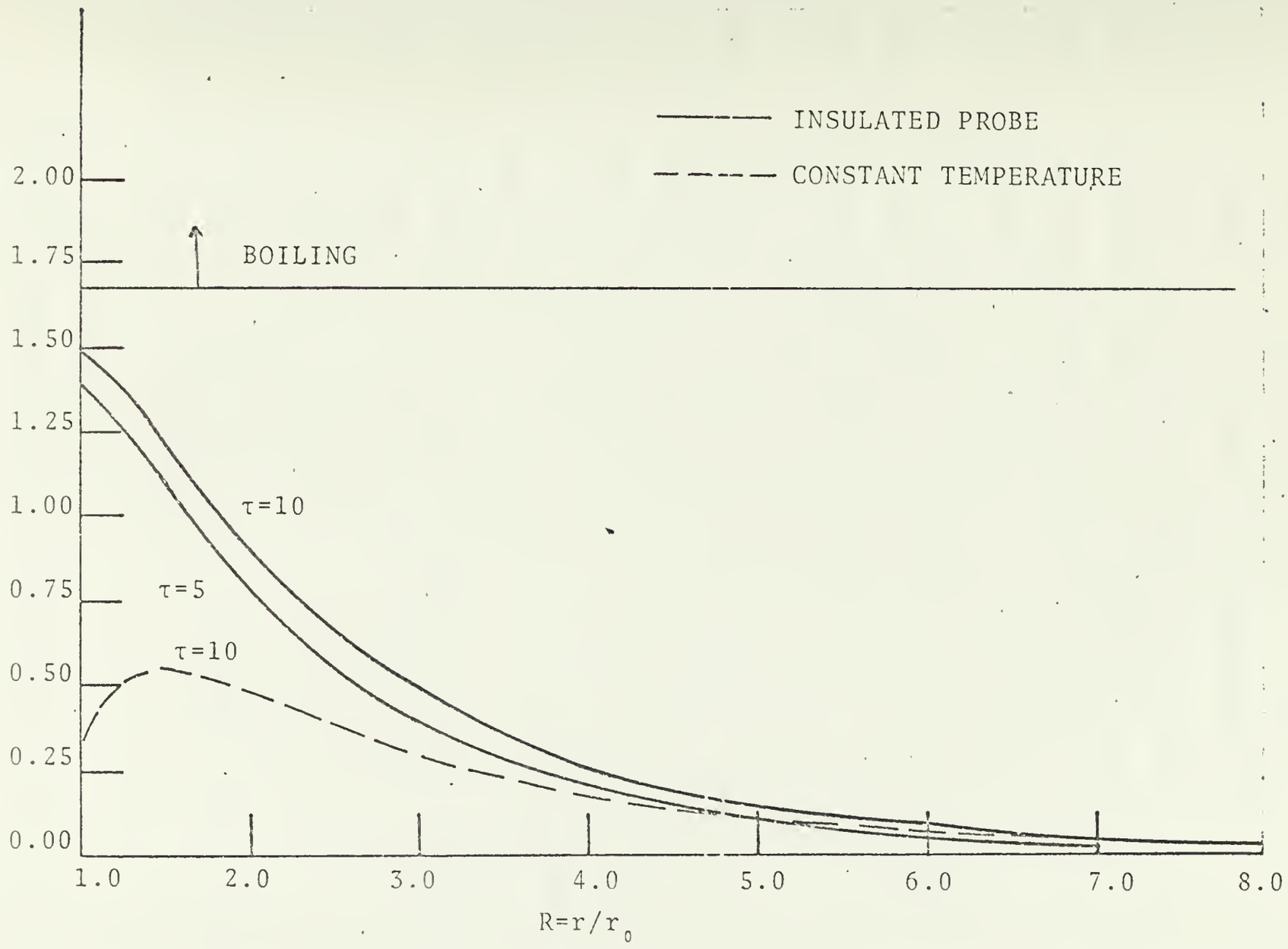

Figure 13. Comparison of Insulated Probe vs. Constant Temperature Probe for $\beta=0.1$, $G=5.0$, Spherical Probe.

be increased without coming close to the boiling temperature. For example, from Figure 12, it is evident that the constant temperature probe (β=0.1, τ=10.0 and G=10.0) produces a lesion of approximately the same size as one depicted in Figure 11 for the insulated probe (β=0.1, τ=10.0 and G=5.0), but the maximum temperature reached by the constant temperature probe is only slightly greater than 70°C whereas the maximum temperature reached by the insulated probe is over 92°C.

Another important factor can be observed from these figures. Recall that if the tissue temperature is kept below 80°C (θ=1.16), only the nervous tissue in the lesion is destroyed while the blood vessels running through the lesion are spared [21]. Note that for all values of G shown for the constant temperature probe, only the nervous tissue is destroyed, whereas for G greater than or equal 5 for the insulated probe, the blood vessels as well as the nervous tissue are destroyed.

One final point to note in regards to the constant temperature probe: not only can the current and time be manipulated to determine the size and maximum temperature of the lesion, but the temperature at which the probe is kept can also be varied. By properly combining these three variables, optimum results can be accomplished.

F. HIGH - RESISTANCE PROBE

The final method to be discussed for producing lesions in the brain is the high-resistance or pure conduction probe.

As was pointed out earlier, this technique consists of passing current through one electrode and using the resistance of the electrode to cause the probe to increase its own temperature, resulting in heat being conducted away from the probe into the surrounding tissue. This heat causes a temperature rise in the tissue and eventually tissue destruction results. Figure 14 shows the resulting temperature field for various values of τ as compared to the insulated probe temperature field. The lesions produced by the high-resistance probe are significantly smaller than those produced by the rf method, but it should be pointed out that the rf lesions have an added amount of uncertainty in that the electrical properties of the region are not that well known, whereas the high-resistance lesion size doesn't depend at all on these electrical properties.

In addition, by properly controlling the temperature of the electrode tip, boiling is not a problem with the high-resistance method. In summary, this method produces safe, predictable and very small lesions.

G. COMPARISON OF MODEL WITH EXPERIMENTAL DATA

An attempt was made to check the proposed model with existing experimental data [1, 3, 5, 6, 13, 28, 35, 36, 37]. However, this attempt proved unsuccessful due to the fact that not all the essential parameters were presented in the reported data. In order to correlate the analytical results with experimental data, it is necessary to know the size of the probe, the current applied, length of application,

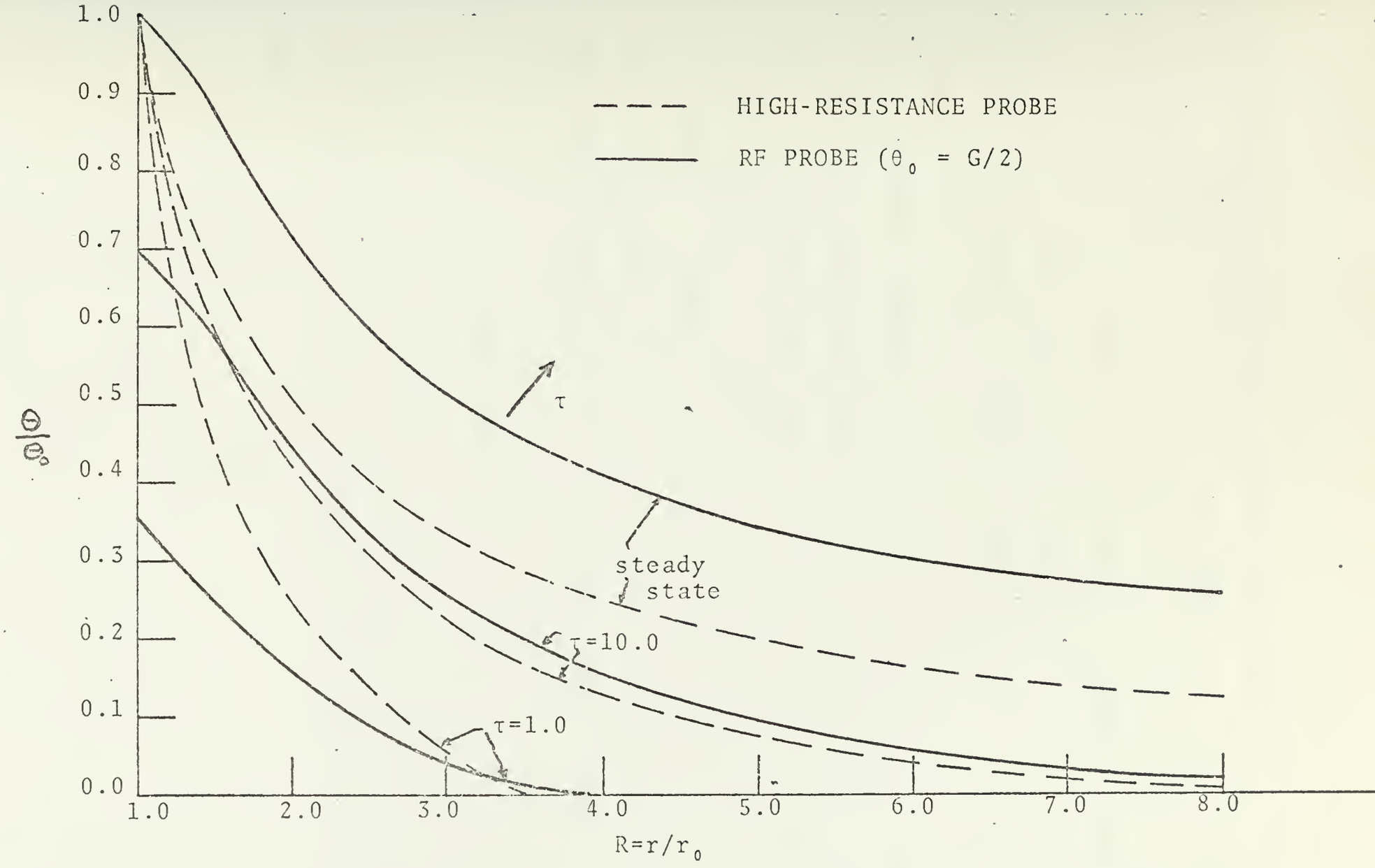

Figure 14. Comparison of High-Resistance Probe vs. rf Heating Probe for Various Values of τ and R, β=0.0.

temperatures recorded and corresponding positions in the brain. At least one of these parameters was either missing or stated unclearly in the reported experimental data.

In order to illustrate this fact, a sample calculation will now be given from the data collected by Aronow [3]. The data consists of a graph of temperature rise versus time of application of current, and a table which gives the maximum temperature recorded, the distance from the electrode at which this maximum temperature was recorded, the power used, and the electrode size. However, it isn't clearly stated whether the electrode size refers to the probe radius or diameter. In addition, one isn't sure of the current used in the experiment. Aronow states that there is an ammeter and a voltmeter on his generator, but he doesn't tabulate the values of current or voltage used.

It will be assumed that the electrode size refers to the probe radius therefore, r_0=0.05 cm. A temperature rise of 45°C is reported at a 0.10 cm distance from the probe and a time of 6 seconds. Therefore, the following data is reported:

r_0 = 0.05 cm

r = 0.10 + 0.05 = 0.15 cm

T = 37 + 45 = 82°C

t = 6 sec.

It will be assumed that

T_0 = 37°C

ρ' = 200 ohm-cm

$$k = 0.0014 \frac{cal}{cm^{\circ}Csec}$$

$$\rho = 1 \frac{gm}{cm^3}$$

$$c = 0.9 \frac{cal}{gm^{\circ}C}$$

$$\alpha = \frac{k}{\rho c} = \frac{0.0014 \frac{cal}{cm^{\circ}Csec}}{\left(1 \frac{gm}{cm^3}\right)\ 0.9\left(\frac{cal}{gm^{\circ}C}\right)} \simeq 0.0016 \frac{cm^2}{sec} .$$

Recall the following non-dimensional variables:

$$R = \frac{r}{r_0} \qquad \beta = \frac{m_b c_b r_0^2}{k} \qquad \tau = \frac{\alpha t}{r_0^2} \qquad \theta = \frac{T - T_0}{T_0} \qquad G = \frac{I^2 \rho'}{16\pi^2 r_0^2 k T_0}$$

An attempt will now be made to substitute the previously mentioned values into the non-dimensional variables and solve for the current.

$$R = \frac{r}{r_0} = \frac{0.15\ cm}{0.05\ cm} = 3$$

$$\theta = \frac{T - T_0}{T_0} = \frac{82-37}{37} \simeq 1.22$$

$$\beta = \frac{m_b c_b r_0^2}{k} = \frac{\left(0.01 \frac{cal}{cm\ ^{\circ}Csec}\right)\left(.05\ cm\right)^2}{\left(0.0014 \frac{cal}{cm\alpha sec}\right)} \simeq 0.018$$

$$\tau = \frac{\alpha t}{r_0^2} = \frac{\left(0.0016 \frac{cm^2}{sec}\right)\left(6\ sec\right)}{(.05cm)^2} \simeq 3.84$$

$$G = \frac{I^2 \rho'}{16\pi^2 r_0^2 k T_0} \Longrightarrow I = \sqrt{\frac{G\ 16\pi^2 r_0^2 k T_0}{\rho'}}$$

Since τ is only 3.84 and β is only 0.018, the effect of blood flow will be neglected in this example. If a larger

probe or a longer time were used, the blood flow effect would play a more important role.

From Table I for an insulated sphere at R=3 and τ=3.84, it can be found that θ/G 0.078.

$$\therefore \quad G = \frac{\theta}{.078} = \frac{1.22}{.078} \simeq 15.6.$$

Now,

$$I = \sqrt{\frac{G\ 16\pi^2 r_0^2 kT_0}{\rho'}}$$

$$I = \sqrt{\frac{(15.6)(16)(\pi^2)(.05\text{cm})^2(.0014\ \frac{\text{cal}}{\text{cm°C sec}})(37°\text{C})}{200\ \Omega\text{cm} \cdot \frac{1\ \text{volt}}{\text{amp}\Omega} \cdot \frac{1\ \text{watt}}{\text{volt amp}} \cdot \frac{.239\ \text{cal}}{\text{watt sec}}}}$$

$$I = \sqrt{67\text{x}10^{-6}\ \text{amp}^2}$$

$$I = \quad 8.2\ \text{ma.}$$

This value for the current appears to be low (Aronow states that a typical value for current in 200 ma). The apparent discrepancy could be due to the fact that the probe size is in fact the diameter, or the distance from the electrode is considered to be the distance from the center of the electrode rather than from the outer radius of the electrode. If the current had been reported, and the vagueness in the above terms eliminated, the data would seem to be more useful.

IV. CONCLUSIONS AND RECOMMENDATIONS

A. CONCLUSIONS

Surgeons are able to produce controlled and predictable spherical lesions in the brain with little or no hemorrhaging and minimal patient discomfort using the radio-frequency technique. However, care must be taken to properly control the amount of current and length of time the current is applied as excessive current or time results in tissue boiling and uncontrolled destruction.

In order to predict lesion size, one must understand the effects of conduction, blood flow, metabolism, and radio-frequency heating on the tissue temperature.

Conduction was found to play a very important role in determining lesion size. The effect of conduction is to distribute the heat away from the probe tip and carry the heat into the brain. The conductive effects very definitely cannot be neglected in attempting to predict lesion size.

The blood flow effect was found to be marginally important in determining the temperature field in the brain. Including the effect of blood flow tends to slightly decrease the temperature continuously throughout the field. Thus, the blood flow convects heat away from the region around the probe. As a result, steady state or equilibrium is reached at an earlier time than if blood flow is neglected. The effect of blood flow becomes more predominant as time is increased. Therefore, if heat is being applied for any substantial amount of time, the effect of blood flow is felt

more strongly. The blood flow parameter, β, is directly proportional to the radius squared. As a result, blood flow plays a more important role in larger probes than for smaller probes. For the probes, currents and times presently used in the radio-frequency technique, the blood flow effects remain marginally important. One would overestimate the lesion size slightly by neglecting these effects.

As the time of heating is increased, the lesion size increases at a decreasing rate until steady state is reached. For a spherical probe of radius 0.05 cm emitting a current of about 20 ma, steady state is reached in about 40 seconds. If a larger probe or a greater current were used, steady state times would be larger.

Increasing the current also results in higher temperatures in the lesion, especially near the probe tip as the majority of heating occurs in this region. As mentioned earlier, excessive current levels result in tissue boiling, whereas if current levels are too low, no tissue destruction occurs.

If the temperature at the probe tip could be maintained at a low enough constant temperature by some cooling mechanism, both the current and the time can be significantly increased, and a controlled well-circumscribed, predictable lesion would result without the ill effects of boiling. The maximum temperature may be moved away from the probe tip and kept well below the boiling point yet high enough to destroy nervous tissue. In addition, the maximum temperature can be

kept low enough so that the blood vessels running through a lesion are spared while the diseased nervous tissue is still destroyed.

The final probe analyzed in the thesis is the high-resistance probe. This probe is also kept at a constant temperature, but the current is used to heat the probe rather than the tissue. As a result, the conductive effect is the only mechanism by which heat is introduced into the surrounding tissue. The lesions produced by this method are significantly smaller than with the rf method. In practice, lesions produced using the high resistance probe should be easier to predict than those created with the rf probe since only the thermal properties of the tissue need be known.

B. RECOMMENDATIONS

It is recommended that experimental work be carried out with both radio-frequency probes and high resistance probes to check the validity of the theoretical models. A thorough literature search revealed sparse data reported; and these data proved to be insufficient to substantiate the model. Not enough parameters are given when data are presented. In order to effectively compare results, it is necessary to include the following parameters when recording data: size of the probe, current applied, time of application, temperatures recorded and corresponding positions in the brain.

It is highly recommended that the constant temperature radio-frequency probe be studied further. In particular,

simple means of cooling the probe tip without greatly increasing the size of the tip must be found. This probe would appear to hold great promise in brain surgery.

APPENDIX A: FINITE DIFFERENCE APPROXIMATION FOR A SPHERICAL PROBE

Statement of non-dimensional equation with boundary conditions and initial condition:

$$\frac{1}{R^2}\frac{\partial\, R^2 \frac{\partial\theta}{\partial R}}{\partial R} - \beta\theta + \frac{G}{R^4} = \frac{\partial\theta}{\partial\tau} \qquad (A.1)$$

(a) $\left.\frac{\partial\theta}{\partial R}\right|_{R=1} = 0.$

(b) As $R\to\infty$, $\theta\to 0$.

(c) At $\tau=0$, $\theta=0$.

where

$$R = \frac{r}{r_0} \qquad \beta = \frac{m_b c_b r_0^2}{k} \qquad \tau = \frac{\alpha t}{r_0^2}$$

$$\theta = \frac{T - T_0}{T_0} \qquad G = \frac{I^2\rho'}{16\pi^2 r_0^2 k T_0} \qquad \phi = \frac{\theta}{G}\ .$$

There seems to be no closed-form solution available for this equation so an explicit, central difference, finite difference technique was used to solve for the temperature field. A discussion of finite difference representation of various terms is given by Ozisik [23]. He examines the finite difference approximation of the terms by using Taylor Series expansions.

Consider a spherical coordinate system with a region interlaced with a R,τ network such that the coordinates of a nodal point (i,n) is given as $R=i\Delta R$ (non-dimensional radial location) and $\tau=n\Delta\tau$ (non-dimensional time). The non-dimensional temperature at time $\tau=n\Delta\tau$ and radial location $R=i\Delta R$ is defined as θ_i^n.

Referencing Özisik [23] the following transformations can be made:

$$\nabla^2\theta = \frac{1}{R}\frac{\partial\left(R^2\frac{\partial\theta}{\partial R}\right)}{\partial R} = \frac{1}{\Delta R^2}\left[\left\{\left(1-\frac{1}{i}\right)\left(\theta^n_{i-1}\right)+\left(1+\frac{1}{i}\right)\left(\theta^n_{i+1}\right)\right\}-2\theta^n_i\right]. \tag{A.2}$$

$$\beta\theta = \beta\theta^n_i . \tag{A.3}$$

$$\frac{G}{R^4} = \frac{G}{(i\Delta R)^4}. \tag{A.4}$$

$$\frac{\partial\theta}{\partial\tau} = \frac{\theta^{n+1}_i - \theta^n_i}{\Delta\tau} . \tag{A.5}$$

Substituting these finite difference approximations into (A.1) yields

$$\frac{1}{\Delta R^2}\left\{\left(1-\frac{1}{i}\right)\theta^n_{i-1}+\left(1+\frac{1}{i}\right)\theta^n_{i+1}\right\}-\frac{2}{\Delta R^2}\theta^n_i-\beta\theta^n_i+\frac{G}{(i\Delta R)^4}$$

$$=\frac{\theta^{n+1}_i-\theta^n_i}{\Delta\tau} . \tag{A.6}$$

Solving for θ^{n+1}_i:

$$\theta^{n+1}_i = \frac{\Delta\tau}{\Delta R^2}\left\{\left(1-\frac{1}{i}\right)\theta^n_{i-1}+\left(1+\frac{1}{i}\right)\theta^n_{i+1}\right\}+\left\{1-\frac{2\Delta\tau}{\Delta R^2}-\beta\Delta\tau\right\}\theta^n_i+\frac{G\Delta\tau}{(i\Delta R)^4} \tag{A.7}$$

Let $M = \frac{\Delta\tau}{\Delta R^2}$

$$\theta^{n+1}_i = M\left\{\left(1-\frac{1}{i}\right)\theta^n_{i-1}+\left(1+\frac{1}{i}\right)\theta^n_{i+1}\right\}+\left\{1-2M-\beta\Delta R^2M\right\}\theta^n_i+\frac{G\,\Delta\tau}{(i\Delta R)^4}. \tag{A.8}$$

The stability criteria serve as a constraint on the problem. A stability condition must be introduced to limit the maximum size of time steps that can be chosen for a fixed ΔR. The stability criteria for this problem will be stated without

proof: $1 - 2M - \beta\Delta R^2 M$ must be ≥ 0 (the interested reader is referred to Özisik [23]).

If $1 - 2M - \beta\Delta R^2 M = 0$

then

$$M = \frac{1}{2 + \beta\Delta R^2} .$$

Recall that $M = \Delta\tau/\Delta R^2$. Choosing ΔR automatically specifies $\Delta\tau$, i.e. $\Delta\tau = M\Delta R^2$. Hence,

$$\theta_i^{n+1} = M\left\{\left(1-\frac{1}{i}\right)\theta_{i-1}^n + \left(1+\frac{1}{i}\right)\theta_{i+1}^n\right\} + \frac{GM\Delta R^2}{(i\Delta R)^4} . \qquad (A.9)$$

Recall from (A.1) that the boundary conditions are

(a) $\left.\frac{\partial\theta}{\partial R}\right|_{R=1} = 0.$

(b) As $R\to\infty$, $\theta\to 0$.

and the initial condition is

(c) At $\tau=0$, $\theta=0$.

Using the finite difference scheme the boundary conditions become

$$\frac{\theta_{i^*+1}^n - \theta_{i^*-1}^n}{2\Delta R} = 0 \quad \text{or} \quad \theta_{i^*-1}^n = \theta_{i^*+1}^n . \qquad (A.10)$$

where i^* corresponds to $R=1.0=i^*\Delta R$,

$$\frac{\theta_{N+1}^n - \theta_{N-1}^n}{2\Delta R} = 0 \quad \text{or} \quad \theta_{N-1}^n = \theta_{N+1}^n \qquad (A.11)$$

where $i = i^*, i^*+1, \ldots, N-1, N$.

The initial condition becomes

$$\theta_i^0 = 0.0. \qquad (A.12)$$

Summary:

Differential equation

$$\theta_i^{n+1} = M\left\{\left(1-\frac{1}{i}\right)\theta_{i-1}^{n} + \left(1+\frac{1}{i}\right)\theta_{i+1}^{n}\right\} + \frac{GM\Delta R^2}{(i\Delta R)^4}. \qquad (A.13)$$

Boundary conditions

(a) $\theta_{i^*-1}^{n} = \theta_{i^*+1}^{n}$

(b) $\theta_{N-1}^{n} = \theta_{N+1}^{n}$.

Initial condition

(c) $\theta_i^{c} = 0.0$.

Computer Program 1 was used to solve this problem. Richardson's Technique [8] was used to test the accuracy of the solution. Three numerical solutions using different sized increments of ΔR were obtained. Because a central difference approximation has a discretization error of the order of ΔR^2 [23], one can plot the approximation to the temperature versus the increment squared (ΔR^2) for each of the three increments used and extrapolate the plot to give the exact solution. Figure A.1 shows Richardson's technique as applied to the spherical program. An increment $\Delta R = 0.1$ proved to be a convenient interval for the program to work with and was well within the limit of accuracy desired by this approximate solution.

An additional problem that was analyzed for this thesis was the case of a constant temperature probe. Recall that this probe serves to lower the maximum temperature incurred

at the probe surface and thereby serves to prevent the tissue from boiling. The differential equation and initial condition remain the same as stated in (A.13). Boundary condition (b) also remains unchanged, but boundary condition (a) is no longer valid. The probe is now considered to have a constant temperature rather than being thermally insulated, or

$$\theta_{i*}^{n} = \text{Constant.} \qquad \text{(A.14)}$$

Computer Program 2 was used to solve this problem.

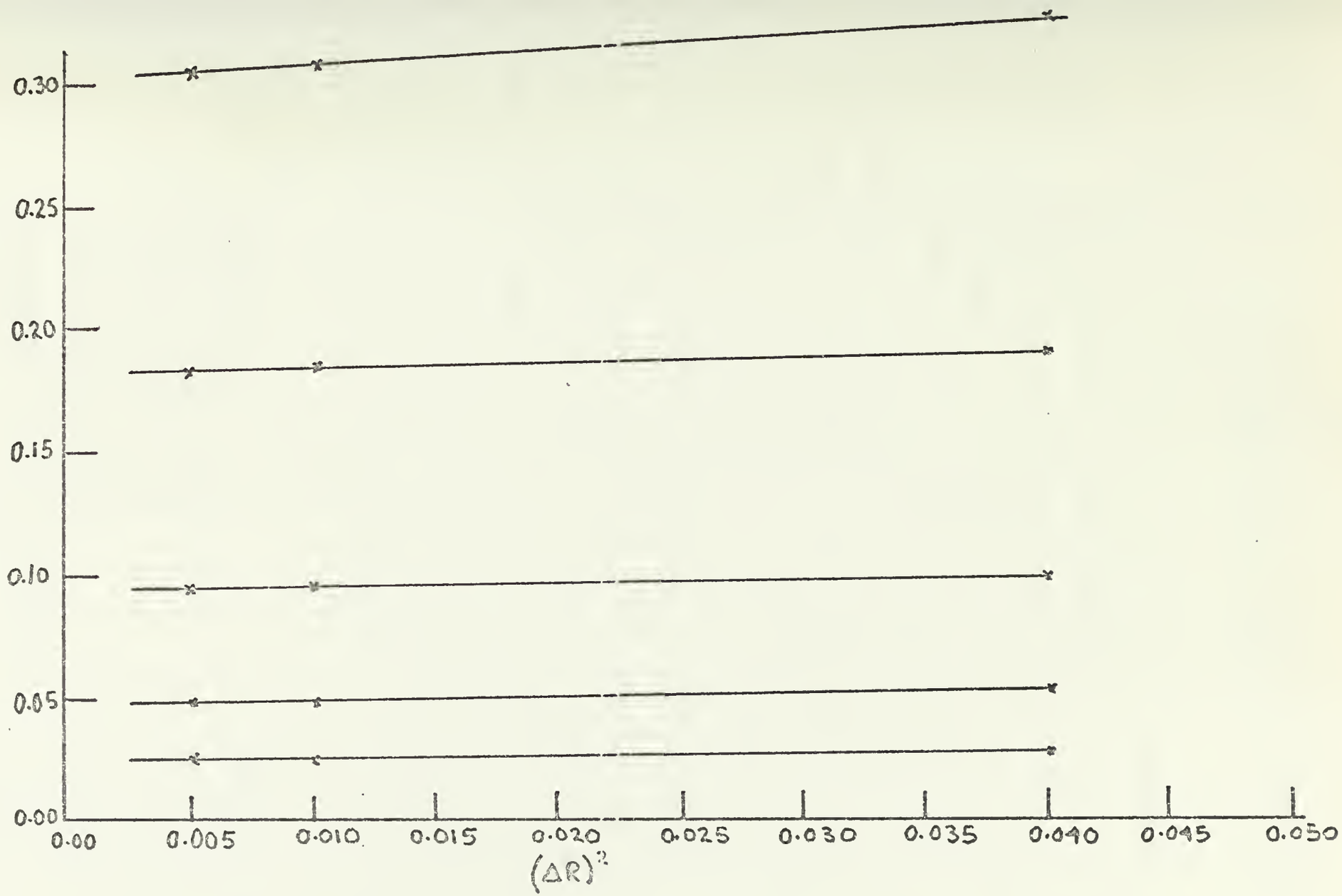

Figure A.1. Richardson's Technique for Spherical Program.

APPENDIX B: COMPLETE SOLUTION FOR THE CYLINDRICAL PROBE

Statement of Problem:

A cylindrical probe of radius "r_0" is embedded in tissue which is initially at a uniform temperature of T_0. Within the tissue there is volumetric heat generation due to metabolism of strength S_m. In addition, there is blood flowing through the medium with a flowrate m_b, specific heat c_b, and temperature T_b. Assume that the length-to-diameter ratio of the probe is large enough so that edge effects may be neglected and assume the tissue is homogeneous and infinite in extent. A radio-frequency current I is emitted from the probe, and the tissue is heated due to the resistivity ρ' of the tissue. Assume that the heat is entirely dissipated in the tissue and that none of the heat is conducted back through the probe, i.e. the probe is thermally insulated. Also, assume that at an infinite distance from the probe, no heat is conducted. Solve for the probe temperature assuming constant properties and one-dimensional radial heat flow.

Notation:

Symbol	Description	Typical Units
α	Tissue thermal diffusivity	cm^2/sec
c	Tissue specific heat	cal/gm/°C
c_b	Blood specific heat	cal/gm/°C
dR	Incremental tissue resistance	ohm
I	Current	amps
k	Thermal conductivity of tissue	cal/cm/sec/°C

Symbol	Description	Typical Units
m_b	Volumetric blood flowrate	$gm/cm^3/sec$
ρ'	Resistivity of tissue	ohm-cm
ρ	Density of tissue	gm/cm^3
r	Radial location in brain	cm
r_0	Probe radius	cm
S_m	Volumetric metabolism rate	$cal/cm^3/sec$
t	Time	sec
T	Tissue temperature	°C
T_b	Temperature of blood	°C
T_0	Initial tissue temperature	°C

Non-dimensional groups:

Temperature $\theta = \frac{T - T_0}{T_0}$ Distance $R = \frac{r}{r_0}$ Time $\tau = \frac{\alpha t}{r_0^2}$

Blood flowrate $\beta = \frac{m_b c_b r_0^2}{k}$ rf heating term $G' = \frac{I^2 \rho'}{4\pi^2 l^2 k T_0}$

Make a one-dimensional energy balance on an element of tissue (see Figure B.1): Heat into element by conduction - Heat out of element by conduction + Volumetric heat generation due to metabolism + Heat input due to blood flow + heat generation due to rf current = Increase in internal energy of element.

Heat in by conduction = $q_{in} = -kA\frac{\partial T}{\partial r} = -k(r\Delta\theta\Delta Z)\frac{\partial T}{\partial r}$

Heat out by conduction = $q_{in} + \frac{\partial q_{in}}{\partial r}\Delta r + \frac{1}{2!}\frac{\partial^2 q_{in}}{\partial r^2}\Delta r^2 + \ldots$

(Taylor Series)

Volumetric heat generation due to metabolism =

$$S_m \Delta V = S_m (r\Delta\theta\Delta r\Delta Z)$$

Heat input due to blood flow =

$$m_b c_b (T_b - T)\Delta V = m_b c_b (r\Delta\theta\Delta r\Delta Z)(T_b - T)$$

Heat generation due to rf heating =

$$I^2 dR = I^2 \frac{\rho' \Delta r}{r\Delta\theta\Delta Z}$$

Increase in internal energy of element =

$$\rho c \frac{\partial T}{\partial t} (r\Delta\theta\Delta r\Delta Z)$$

Combining the above

$$- \frac{\partial q_{in}}{\partial r} \Delta r + \frac{I^2 \rho' \Delta r}{r\Delta\theta\Delta Z} + m_b c_b (T_b - T) r\Delta\theta\Delta r\Delta Z + S_m (r\Delta\theta\Delta r\Delta Z)$$

$$= \rho c r \Delta\theta\Delta r\Delta Z + O(\Delta r^2) \qquad (B.1)$$

or by dividing by Δr and taking the limit as $\Delta r \to 0$

$$- \frac{\partial q_{in}}{\partial r} + \frac{I^2 \rho'}{r\Delta\theta\Delta Z} + m_b c_b (T_b - T) r\Delta\theta\Delta Z + S_m r\Delta\theta\Delta Z = \rho c \frac{\partial T}{\partial t} r\Delta\theta\Delta Z. \qquad (B.2)$$

Recall $q_{in} = -kr\Delta\theta\Delta Z \frac{\partial T}{\partial r}$

$$\frac{\partial (kr\Delta\theta\Delta Z \frac{\partial T}{\partial r})}{\partial r} + \frac{I^2 \rho'}{r\Delta\theta\Delta Z} + m_b c_b (T_b - T) r\Delta\theta\Delta Z + S_m r\Delta\theta\Delta Z$$

$$= \rho c \frac{\partial T}{\partial t} r\Delta\theta\Delta Z. \qquad (B.3)$$

Dividing through by $r\Delta\theta\Delta Z$

$$\frac{1}{r} \frac{\partial \left(kr \frac{\partial T}{\partial r}\right)}{\partial r} + S_m + \frac{I^2 \rho'}{r^2 \Delta\theta^2 \Delta Z^2} + m_b c_b (T_b - T) = \rho c \frac{\partial T}{\partial t}. \qquad (B.4)$$

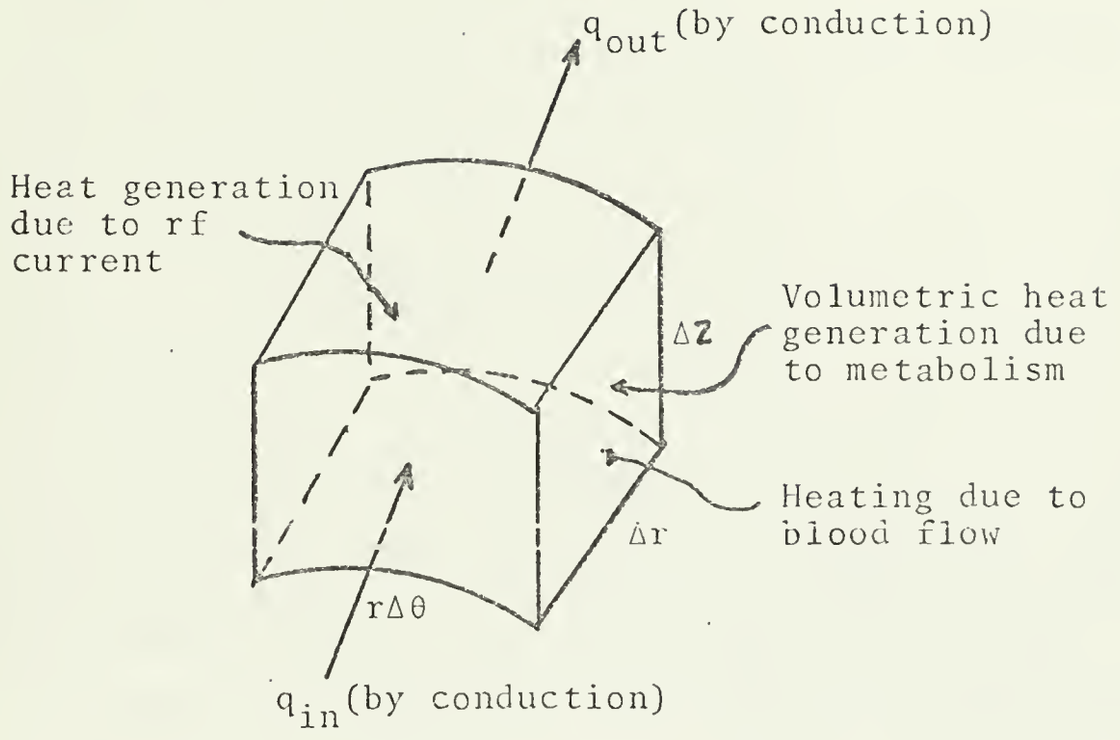

Figure B.1. One-dimensional Energy Balance on a Cylindrical Element.

For a constant k (B.4) reduces to

$$\frac{k}{r}\frac{\partial\left(r\frac{\partial T}{\partial r}\right)}{\partial r} + S_m + \frac{I^2\rho'}{r^2\Delta\theta^2\Delta Z^2} + m_b c_b(T_b - T) = \rho c\frac{\partial T}{\partial t}. \quad (B.5)$$

At this point a further constraint will be placed on the system. Prior to the insertion of the probe it will be assumed that the temperature of the medium is constant. In addition, it will be assumed that metabolism and blood flow have been active long before the insertion of the probe.

If this be the case, then

$$S_m = m_b c_b(T_0 - T)$$

or

$$T_0 = T_b + S_m/m_b c_b.$$

This implies that the medium temperature is warmer than the fluid by an amount $S_m/m_b c_b$ prior to the insertion of the probe. At steady state the fluid thus removes the heat added by the volumetric heat source.

Putting Equation (B.5) in the form

$$\frac{k}{r}\frac{\partial\left(r\frac{\partial T}{\partial r}\right)}{\partial r} + m_b c_b\left\{\left(T_b - \frac{S_m}{m_b c_b}\right) - T\right\} + \frac{I^2\rho'}{r^2\Delta\theta^2\Delta Z^2} = \rho c\frac{\partial T}{\partial t}. \quad (B.6)$$

suggests substituting T_0 for $(T_b + S_m/m_b c_b)$. When this is done, Equation (B.6) reads

$$\frac{k}{r}\frac{\partial\left(r\frac{\partial T}{\partial r}\right)}{\partial r} + m_b c_b(T_0 - T) + \frac{I^2\rho'}{r^2\Delta\theta^2\Delta Z^2} = \rho c\frac{\partial T}{\partial t}. \quad (B.7)$$

Let $\Delta\theta = 2\pi$ and $\Delta Z = 1$ to get

$$\frac{k}{r}\frac{\partial\left(r\frac{\partial T}{\partial r}\right)}{\partial r} + m_b c_b (T_0 - T) + \frac{I^2\rho'}{4r^2\pi^2 l^2} = \rho c \frac{\partial T}{\partial t} . \qquad (B.8)$$

Now, to cast (B.8) into non-dimensional form let

$$R = \frac{r}{r_0} \quad \beta = \frac{m_b c_b r_0^2}{k} \quad \tau = \frac{\alpha t}{r_0^2} \quad \theta = \frac{T - T_0}{T_0} \quad G' = \frac{I^2\rho'}{4\pi^2 l^2 k T_0}$$

Substituting the above non-dimensional quantities into Equation (B.8) gives

$$\frac{1}{R}\frac{\partial\left(R\frac{\partial\theta}{\partial R}\right)}{\partial R} - \beta\theta + \frac{G'}{R^2} = \frac{\partial\theta}{\partial\tau} . \qquad (B.9)$$

Equation (B.9) is the equation that must be solved in order to describe the temperature of the tissue as a function of time when a radio-frequency current is emitted from a probe embedded in a medium with a volumetric heat source and a flowing fluid. In order to solve the problem, boundary conditions and an initial condition must be stated. The boundary and initial conditions are as follows:

(a) None of the heat generated due to rf current in the tissue is conducted into the probe (probe is thermally insulated);

AT $r = r_0$, $\frac{\partial T}{\partial r} = 0$

or, in non-dimensional form

at $R = 1$, $\partial\theta/\partial R = 0$;

(b) as $r\to\infty$, the medium remains unaffected

as $r\to\infty$, $T\to T_0$

or, in non-dimensional form

as $R\to\infty$, $\theta\to 0$;

(c) at time $t = 0$, $T = T_0$

or, in non-dimensional form

at $\tau = 0$, $\theta = 0$.

Summary

Differential equation

$$\frac{1}{R}\frac{\partial\left(R\frac{\partial\theta}{\partial R}\right)}{\partial R} - \beta\theta + \frac{G'}{R^2} = \frac{\partial\theta}{\partial\tau} . \qquad (B.10)$$

Boundary conditions

$$\left.\frac{\partial\theta}{\partial R}\right|_{R=1} = 0 \qquad (B.11)$$

$$\text{as } R\to\infty,\ \theta\to 0. \qquad (B.12)$$

Initial condition

$$\text{at } \tau = 0,\ \theta = 0.$$

Solution

An explicit, central difference, finite difference approximation was used to solve for the temperature field. Consider a cylindrical coordinate system interlaced with a R,τ network such that the non-dimensional temperature at a time $\tau=n\tau$ and radial location $R=i\Delta R$ is defined as θ_i^n, where $n=1,2,\ldots$, and $i=i^*, i^*+1,\ldots,N-1, N$, and i^* is the location where $R=1.0$.

Referring to Ozisik [23] the following transformations can be made:

$$\nabla^2\theta = \frac{1}{R}\frac{\partial\left(R\frac{\partial\theta}{\partial R}\right)}{\partial R} = \frac{1}{\Delta R^2}\left\{\left(1-\frac{1}{2i}\right)\theta_{i-1}^n + \left(1+\frac{1}{2i}\right)\theta_{i+1}^n - 2\theta_i^n\right\} \qquad (B.14)$$

$$\beta\theta = \beta\theta_i^n \tag{B.15}$$

$$\frac{G'}{R^2} = \frac{G'}{(i\Delta R)^2} \tag{B.16}$$

$$\frac{\partial\theta}{\partial\tau} = \frac{\theta_i^{n+1} - \theta_i^n}{\Delta\tau} . \tag{B.17}$$

Substituting these finite difference approximations into (B.10) gives

$$\frac{1}{\Delta R^2}\left\{\left(1-\frac{1}{2i}\right)\theta_{i-1}^n + \left(1+\frac{1}{2i}\right)\theta_{i+1}^n\right\} - \frac{2}{\Delta R^2}\theta_i^n + \frac{G'}{(i\Delta R)^2}$$

$$= \frac{\theta_i^{n+1} - \theta_i^n}{\Delta\tau} \tag{B.18}$$

Solving for θ_i^{n+1} gives

(B.19)

$$\theta_i^{n+1} = \frac{\Delta\tau}{\Delta R^2}\left\{\left(1-\frac{1}{2i}\right)\theta_{i-1}^n + \left(1+\frac{1}{2i}\right)\theta_{i+1}^n\right\} + \left\{1-\frac{2\Delta\tau}{\Delta R^2} - \beta\Delta\tau\right\}\theta_i^n + \frac{G'\Delta\tau}{(i\Delta R)^2}.$$

Let $M = \Delta\tau/\Delta R^2$

(B.20)

$$\theta_i^{n+1} = M\left\{\left(1-\frac{1}{2i}\right)\theta_{i-1}^n + \left(1+\frac{1}{2i}\right)\theta_{i+1}^n\right\} + \left\{1-2M-\beta\Delta R^2 M\right\}\theta_i^n + \frac{G'\Delta\tau}{(i\Delta R)^2}.$$

To maintain the stability criteria [23],

$$1 - 2M - \beta\Delta R^2 M = 0 \tag{B.21}$$

then

$$M = \frac{1}{2 + \beta\Delta R^2} \tag{B.22}$$

Recall $M = \Delta\tau/\Delta R$. Choosing ΔR automatically specifies $\Delta\tau$, i.e. $\Delta\tau = M\Delta R^2$. Hence,

(B.23)

$$\theta_i^{n+1} = M\left\{\left(1-\frac{1}{2i}\right)\theta_{i-1}^n + \left(1+\frac{1}{2i}\right)\theta_{i+1}^n\right\} + \frac{G'M}{i^2}$$

Recall the boundary conditions from (B.11) and (B.12)

(a) $\left.\frac{\partial\theta}{\partial R}\right|_{R=1} = 0$

(b) as $R\to\infty$, $\theta\to 0$.

Using the finite difference scheme, the boundary conditions become

$$\frac{\theta^n_{i^*+1} - \theta^n_{i^*+1}}{2\Delta R} = 0 \quad \text{or} \quad \theta^n_{i^*-1} = \theta^n_{i^*+1} \tag{B.24}$$

$$\frac{\theta^n_{N+1} - \theta^n_{N-1}}{2\Delta R} = 0 \quad \text{or} \quad \theta^n_{N-1} = \theta^n_{N+1} \tag{B.25}$$

where $i = i^*, i^*+1, \ldots, N-1, N$, and i^* corresponds to $R = 1.0$. The initial condition becomes

$$\theta^0_i = 0.0. \tag{B.26}$$

Summary

Differential equation

$$\theta^{n+1}_i = M\left\{\left(1-\frac{1}{2i}\right)\theta^n_{i-1} + \left(1+\frac{1}{2i}\right)\theta^n_{i+1}\right\} + \frac{G'M}{i^2}. \tag{B.27}$$

Boundary conditions

(a) $\theta^n_{i^*-1} = \theta^n_{i^*+1}$

(b) $\theta^n_{N-1} = \theta^n_{N+1}$.

Initial condition

(c) $\theta^0_i = 0.0.$

By specifying β, the blood flow factor, and ΔR, the increment, M can be found and $\Delta\tau$ can be found. Computer Program

3 does this and also solves for the temperature at various times and locations. Richardson's technique [8] was used to check the accuracy of the program. Figure B.2 shows Richardson's technique as it applied to the cylindrical program.

As with the spherical probe, the constant temperature boundary condition was analyzed with the cylindrical probe. The only difference to the problem as stated in the previous summary is boundary condition (a). This boundary condition becomes

$$\theta_{i*}^{n} = \text{Constant.} \qquad \text{(B.28)}$$

Computer Program 4 was used to solve this problem.

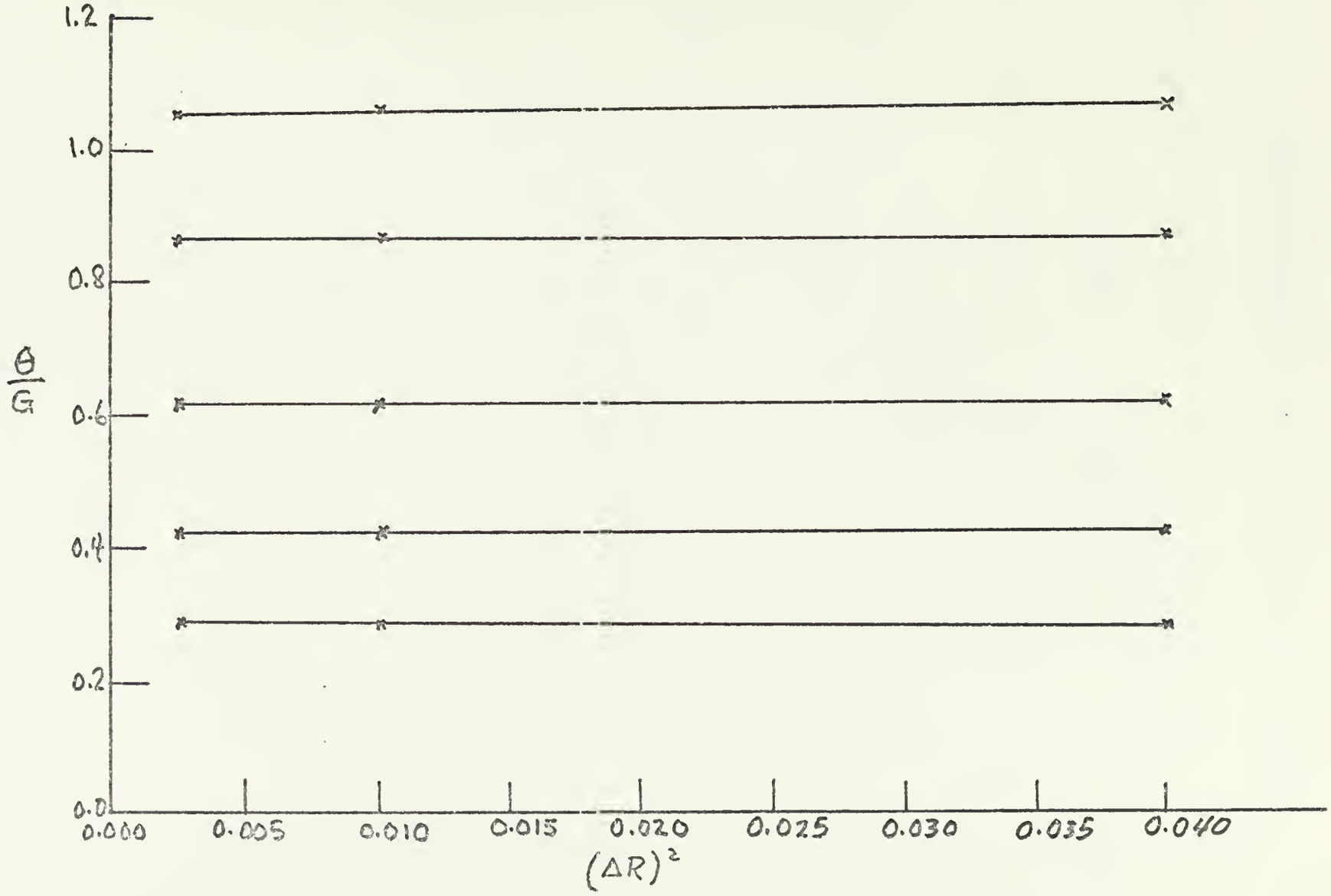

Figure B.2. Richardson's Technique for a Cylindrical Program.

APPENDIX C: SOLUTION FOR THE HIGH-RESISTANCE SPHERICAL HEATING PROBE

Differential equation

$$\frac{1}{R^2}\frac{\partial\left(R^2\frac{\partial\theta}{\partial R}\right)}{\partial R} - \beta\theta = \frac{\partial\theta}{\partial\tau} . \qquad (C.1)$$

Boundary conditions

At $R = 1$, $\theta = \theta_0$ (a constant) (C.2)

As $R\to\infty$, $\theta\to 0$. (C.3)

Initial condition

At $\tau = 0$, $\theta = 0$. (C.4)

Expanding (C.1) gives

$$\frac{2}{R}\frac{\partial\theta}{\partial R} + \frac{\partial^2\theta}{\partial R^2} - \beta\theta = \frac{\partial\theta}{\partial\tau}. \qquad (C.5)$$

Using a change of variables technique as described in Carslaw and Jaeger [7], let $\theta = v/R$.

Then,

$$\frac{\partial\theta}{\partial R} = \frac{\partial\left(\frac{v}{R}\right)}{\partial R} = -\frac{v}{R^2} + \frac{1}{R}\frac{\partial v}{\partial R}. \qquad (C.6)$$

$$\frac{\partial^2\theta}{\partial R^2} = \frac{2v}{R^3} - \frac{1}{R^2}\frac{\partial v}{\partial R} - \frac{1}{R^2}\frac{\partial v}{\partial R} + \frac{1}{R}\frac{\partial^2 v}{\partial R^2} . \qquad (C.7)$$

or

$$\frac{\partial^2\theta}{\partial R^2} = \frac{2v}{R^3} - \frac{2}{R^2}\frac{\partial v}{\partial R} + \frac{1}{R}\frac{\partial^2 v}{\partial R^2} .$$

Substituting these new variables into (C.5) yields

$$-\frac{2v}{R^3} + \frac{2}{R^2}\frac{\partial v}{\partial R} + \frac{2v}{R^3} - \frac{2}{R^2}\frac{\partial v}{\partial R} + \frac{1}{R}\frac{\partial^2 v}{\partial R^2} - \beta\frac{v}{R} = \frac{1}{R}\frac{\partial v}{\partial\tau}$$

$$\frac{1}{R}\frac{\partial^2 v}{\partial R^2} - \beta\frac{v}{R} = \frac{1}{R}\frac{\partial v}{\partial\tau} . \qquad (C.8)$$

Multiplying through by R

$$\frac{\partial^2 v}{\partial R^2} - \beta v = \frac{\partial v}{\partial \tau} \quad . \tag{C.9}$$

From Carslaw and Jaeger [7], p. 134, the solution to this equation is

$$v = \frac{1}{2} V_0 e^{-\sqrt{\beta}\,(R-1)} \left\{ \operatorname{erfc} \frac{(R-1)}{2\sqrt{\tau}} - \sqrt{\beta\tau} \right\} + e^{\sqrt{\beta}\,(R-1)} \operatorname{erfc} \left\{ \frac{(R-1)}{2\sqrt{\tau}} + \sqrt{\beta\tau} \right\} \tag{C.10}$$

or

$$\frac{\theta}{\theta_0} = \frac{1}{2R} \left[e^{-\sqrt{\beta}\,(R-1)} \left\{ \operatorname{erfc} \frac{(R-1)}{2\sqrt{\tau}} - \sqrt{\beta\tau} \right\} + e^{\sqrt{\beta}\,(R-1)} \operatorname{erfc} \left\{ \frac{(R-1)}{2\sqrt{\tau}} + \sqrt{\beta\tau} \right\} \right] \tag{C.11}$$

This equation was solved using Computer Program 5. The results are shown on Figure 14.

The steady state solution can be obtained directly:

$$\frac{\partial^2 v}{\partial R^2} - \beta v = 0 \Rightarrow v = C_1 e^{-\sqrt{\beta}\,(R-1)} + C_2 e^{\sqrt{\beta}\,(R-1)}$$

Applying boundary condition (C.3)

As $R \to \infty$, $\theta \to 0 \Rightarrow C_2 = 0$

$$\therefore \quad \theta = \frac{C_1}{R} e^{-\sqrt{\beta}\,(R-1)}$$

At $R = 1$, $\theta = \theta_0 \Rightarrow C_1 = \theta_0$

$$\therefore \quad \frac{\theta}{\theta_0} = \frac{e^{-\sqrt{\beta}\,(R-1)}}{R}$$

A comparison of the high-resistance program and the finite difference program for the constant temperature probe (taking G = 0) serves as an additional check on the finite difference program. Figure C.1 shows this comparison. As the graph depicts, the two solutions fall exactly on one another, thus giving additional assurance to the previous programs.

When comparing the lesion size of the high-resistance technique with the lesion size of the insulated rf technique, it is desirable to compare the size at steady state values. In order to do this, the rf probe must be fixed so that it has the same tip temperature as a comparable sized high-resistance probe at steady state, (see Figure 14). This tip temperature can be attained provided a proper value is chosen for the radio-frequency term G. Recall that for the rf probe the problem is as follows:

Differential equation

$$\frac{1}{R^2} \frac{\partial \left(R^2 \frac{\partial \theta}{\partial R}\right)}{\partial R} - \beta\theta + \frac{G}{R^4} = \frac{\partial \theta}{\partial \tau} .$$

Boundary conditions

At $R = 1$, $\frac{\partial \theta}{\partial R} = 0$.

As $R \to \infty$, $\theta \to 0$.

Initial condition

At $\tau = 0$, $\theta = 0$.

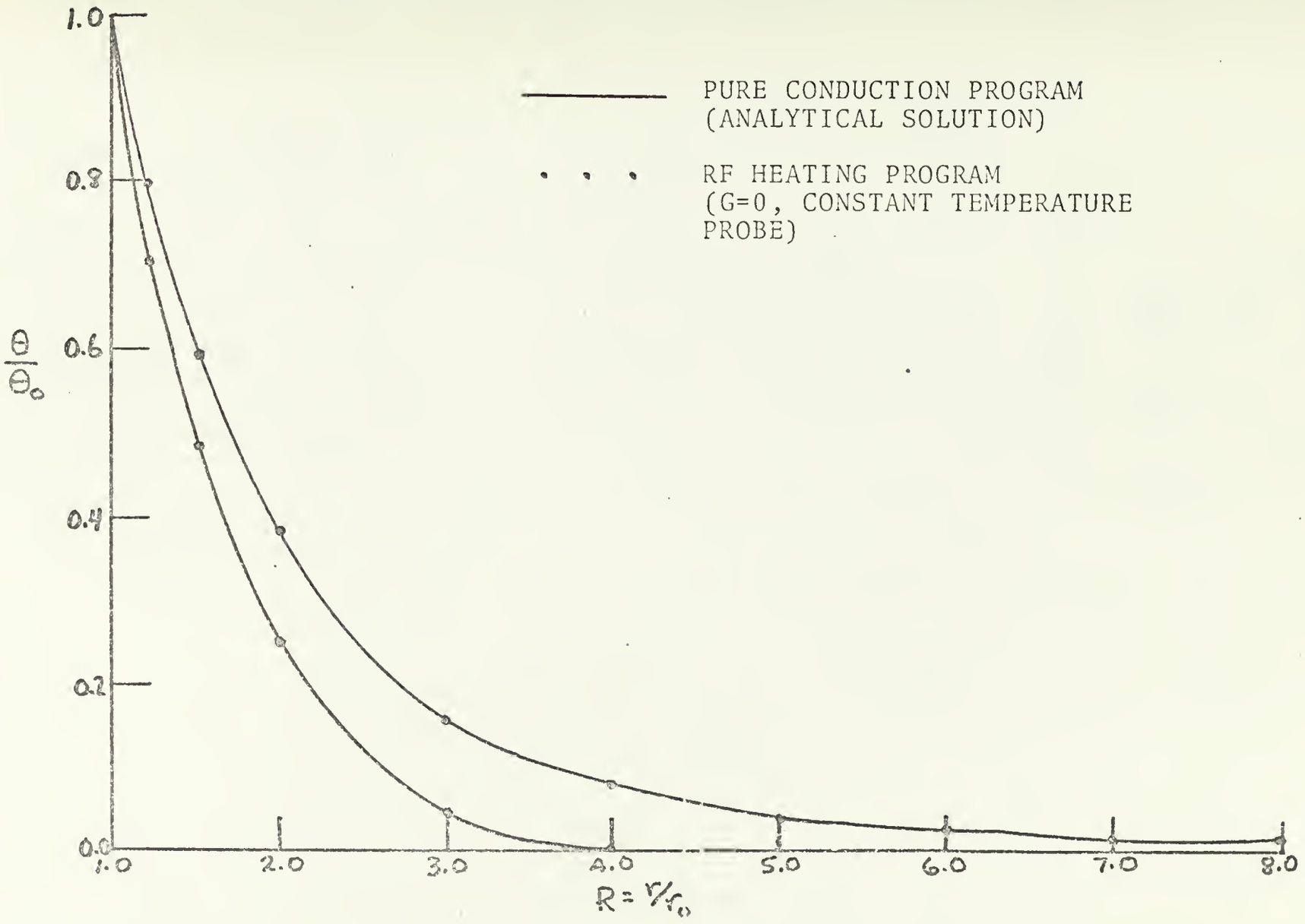

Figure C.1. Comparison of Pure Conduction Program with rf Heating Program (Constant Temperature Probe, G=0), β=0.1.

Neglect blood flow and assume steady state

$$\frac{\partial\left(R^2\frac{\partial\theta}{\partial R}\right)}{\partial R} = -\frac{G}{R^2}$$

$$R^2\frac{\partial\theta}{\partial R} = \frac{G}{R} + C_1$$

$$\frac{\partial\theta}{\partial R} = \frac{G}{R^3} + \frac{C_1}{R^2}\ .$$

But at $R = 1$, $\frac{\partial\theta}{\partial R} = 0 \Rightarrow C_1 = -G$

$$\therefore\ \frac{\partial\theta}{\partial R} = \frac{G}{R^3} - \frac{G}{R^2}$$

$$\theta = -\frac{G}{2R^2} + \frac{1}{R} + C_2.$$

But as $R\to\infty$, $\theta\to 0 \Rightarrow C_2 = 0$

$$\therefore\ \theta = -\frac{G}{2R^2} + \frac{G}{R}$$

At $R = 1$, $\theta = \theta_0 = \frac{T_w - T_0}{T_0}$

$$\therefore\ \theta_0 = \frac{G}{2}\ .$$

In Figure 14 θ is plotted versus R. Once θ_0 is chosen, one can find a value for G that will result in the steady state temperature of the two probes being the same at the probe tip.

```
C       COMPUTER PROGRAM 1
C       PROGRAM FOR THE INSULATED SPHERE

        DIMENSION TET(500,2)
        ITIME=0
        READ (5,100)BETA,G,DR,LI,IH
  100   FORMAT (3F10.0,2I10)
        WRITE (6,150)BETA,DR,G,LI,IH
  150   FORMAT (' ',T4,'BETA=',F4.2,5X,'DR=',F6.4,5X,'G=',F6.1
        ,5X,'LI=',I3,5X,'IH=',I4)
        WRITE (6,2000)
 2000   FORMAT ('1',T4,'TEMPERATURE DISTRIBUTION AT SPECIFIED
        TIME AND RADIAL LOCATIONS'//' ',T8,'TIME(TAU)',T22,'LO
        CATION(R)',T42,'TEMPERATURE(THETA)')
        EM=1.0/(2.0+BETA*DR**2)
        DELTAU=EM*DR**2
        DO 10 K=1,IH
   10   TET(K,1)=0.0
   50   DO 200 I=LI,IH
        TET(IH+1,1)=TET(IH-1,1)
        TET(LI-1,1)=TET(LI+1,1)
        X=I
  200   TET(I,2)=EM*((1.-1./X)*TET(I-1,1)+(1.+1./X)*TET(I+1,1)
        )+G*EM*DR**2/((X*DR)**4)
        ITIME=ITIME+1
        TAU=ITIME*DELTAU
        IF(ITIME.GT.1000)GO TO 90
        IF (ITIME.GT.100)GO TO 70
        ITEST=ITIME/20*20
        GO TO 80
   70   ITEST=ITIME/50*50
        GO TO 80
   90   ITEST=ITIME/100*100
   80   J=0
        DO 60 J=LI,IH
        R=J*DR
        IF ((ITIME-ITEST).NE.0)GO TO 60
        WRITE(6,220)TAU,R,TET(J,2)
  220   FORMAT (' ',F15.4,7X,F6.3,5X,E15.7)
   60   TET(J,1)=TET(J,2)
        IF (ITIME.GT.4000)STOP
        GO TO 50
        END
```

```
C       COMPUTER PROGRAM 2
C       PROGRAM FOR THE CONSTANT TEMPERATURE SPHERE

        DIMENSION TET(500,2)
        ITIME=0
        READ (5,100)BETA,G,DR,LI,IH
  100   FORMAT (3F10.0,2I10)
        WRITE (6,150)BETA,DR,G,LI,IH
  150   FORMAT (' ',T4,'BETA=',F4.2,5X,'DR=',F6.4,5X,'G=',F6.1
       ,5X,'LI=',I3,5X,'IH=',I4)
        WRITE (6,2000)
 2000   FORMAT ('1',T4,'TEMPERATURE DISTRIBUTION AT SPECIFIED
       TIME AND RADIAL LOCATIONS'//' ',T8,'TIME(TAU)',T22,'LO
       CATION(R)',T42,'TEMPERATURE(THETA)')
        EM=1.0/(2.0+BETA*DR**2)
        DELTAU=EM*DR**2
        DO 10 K=1,IH
   10   TET(K,1)=0.0
        TET(10,1)=0.3
        TET(10,2)=0.3
   50   DO 200 I=LI,IH
        TET(IH+1,1)=TET(IH-1,1)
        X=I
  200   TET(I,2)=EM*((1.-1./X)*TET(I-1,1)+(1.+1./X)*TET(I+1,1)
       )+G*EM*DR**2/((X*DR)**4)
        ITIME=ITIME+1
        TAU=ITIME*DELTAU
        IF(ITIME.GT.1000)GO TO 90
        IF (ITIME.GT.100)GO TO 70
        ITEST=ITIME/20*20
        GO TO 80
   70   ITEST=ITIME/50*50
        GO TO 80
   90   ITEST=ITIME/100*100
   80   J=0
        LM=LI-1
        DO 60 J=LM,IH
        R=J*DR
        IF ((ITIME-ITEST).NE.0)GO TO 60
        WRITE(6,220)TAU,R,TET(J,2)
  220   FORMAT (' ',F15.4,7X,F6.3,5X,E15.7)
   60   TET(J,1)=TET(J,2)
        IF (ITIME.GT.4000)STOP
        GO TO 50
        END
```

```
C       COMPUTER PROGRAM 3
C       PROGRAM FOR THE INSULATED CYLINDER

        DIMENSION TET(500,2)
        ITIME=0
        READ (5,100)BETA,G,DR,LI,IH
  100   FORMAT (3F10.0,2I10)
        WRITE (6,150)BETA,DR,G,LI,IH
  150   FORMAT (' ',T4,'BETA=',F4.2,5X,'DR=',F6.4,5X,'G=',F6.1
        ,5X,'LI=',I3,5X,'IH=',I4)
        WRITE (6,2000)
 2000   FORMAT ('1',T4,'TEMPERATURE DISTRIBUTION AT SPECIFIED
        TIME AND RADIAL LOCATIONS'//' ',T8,'TIME(TAU)',T22,'LO
        CATION(R)',T42,'TEMPERATURE(THETA)')
        EM=1.0/(2.0+BETA*DR**2)
        DELTAU=EM*DR**2
        DO 10 K=1,IH
    10  TET(K,1)=0.0
    50  DO 200 I=LI,IH
        TET(IH+1,1)=TET(IH-1,1)
        TET(LI-1,1)=TET(LI+1,1)
        X=I
   200  TET(I,2)=EM*((1.-1./(2.*X))*TET(I-1,1)+(1.+1./(2.*X))*
        TET(I+1,1))+G*EM/(X**2)
        ITIME=ITIME+1
        TAU=ITIME*DELTAU
        IF(ITIME.GT.1000)GO TO 90
        IF (ITIME.GT.100)GO TO 70
        ITEST=ITIME/20*20
        GO TO 80
    70  ITEST=ITIME/50*50
        GO TO 80
    90  ITEST=ITIME/100*100
    80  J=0
        DO 60 J=LI,IH
        R=J*DR
        IF ((ITIME-ITEST).NE.0)GO TO 60
        WRITE(6,220)TAU,R,TET(J,2)
   220  FORMAT (' ',F15.4,7X,F6.3,5X,E15.7)
    60  TET(J,1)=TET(J,2)
        IF (ITIME.GT.4000)STOP
        GO TO 50
        END
```

```
C       COMPUTER PROGRAM 4
C       PROGRAM FOR THE CONSTANT TEMPERATURE CYLINDER

        DIMENSION TET(500,2)
        ITIME=0
        READ (5,100)BETA,G,DR,LI,IH
  100   FORMAT (3F10.0,2I10)
        WRITE (6,150)BETA,DR,G,LI,IH
  150   FORMAT (' ',T4,'BETA=',F4.2,5X,'DR=',F6.4,5X,'G=',F6.1
        ,5X,'LI=',I3,5X,'IH=',I4)
        WRITE (6,2000)
 2000   FORMAT ('1',T4,'TEMPERATURE DISTRIBUTION AT SPECIFIED
        TIME AND RADIAL LOCATIONS'//' ',T8,'TIME(TAU)',T22,'LO
        CATION(R)',T42,'TEMPERATURE(THETA)')
        EM=1.0/(2.0+BETA*DR**2)
        DELTAU=EM*DR**2
        DO 10 K=1,IH
    10  TET(K,1)=0.0
        TET(10,1)=1.0
        TET(10,2)=1.0
    50  DO 200 I=LI,IH
        TET(IH+1,1)=TET(IH-1,1)
        X=I
   200  TET(I,2)=EM*((1.-1./(2.*X))*TET(I-1,1)+(1.+1./(2.*X))*
        TET(I+1,1))+G*EM/(X**2)
        ITIME=ITIME+1
        TAU=ITIME*DELTAU
        IF(ITIME.GT.1000)GO TO 90
        IF (ITIME.GT.100)GO TO 70
        ITEST=ITIME/20*20
        GO TO 80
    70  ITEST=ITIME/50*50
        GO TO 80
    90  ITEST=ITIME/100*100
    80  J=0
        LM=LI-1
        DO 60 J=LM,IH
        R=J*DR
        IF ((ITIME-ITEST).NE.0)GO TO 60
        WRITE(6,220)TAU,R,TET(J,2)
   220  FORMAT (' ',F15.4,7X,F6.3,5X,E15.7)
    60  TET(J,1)=TET(J,2)
        IF (ITIME.GT.4000)STOP
        GO TO 50
        END
```

```
C       COMPUTER PROGRAM 5
C       PROGRAM FOR THE HIGH-RESISTANCE SPHERE

        DIMENSION TET(500)
        READ (5,100) BETA,THETO,IH
  100   FORMAT (2F10.0,I10)
        WRITE (6,150) BETA,THETO,IH
  150   FORMAT (' ',T4,'BETA=',F8.4,5X,'THETO=',F10.1,5X,'IH='
       ,I5)
 2000   FORMAT ('1',T4,'TEMPERATURE DISTRIBUTION AT SPECIFIED
       TIME AND RADIAL LOCATIONS'//' ',T8,'TIME(TAU)',T22,'LO
       CATION(R)',T42,'TEMPERATURE(THETA)')
        SQBET=SQRT(BETA)
        TAU=0.2
   50   SQTAU=SQRT(TAU)
        DR=0.2
        BTAU=BETA*TAU
        SQBTAU=SQRT(BTAU)
        DO 200 I=1,IH
   12   R=I*DR
        EX=SQBET*(R-1.0)
        EXNEG=-EX
        A=(R-1.0)/(2.0*SQTAU)-SQBTAU
        B=(R-1.0)/(2.0*SQTAU)+SQBTAU
   11   TET(I)=THETO*(1./(2.0*R)*(EXP(EXNEG)*ERFC(A)+EXP(EX)*E
       RFC(B)))
        WRITE (6,220) TAU,R,TET(I)
  220   FORMAT (' ',F15.4,7X,F6.3,5X,E15.7)
  200   CONTINUE
        IF(TAU.GT.2.0) GO TO 13
        GO TO 14
   13   TAU=TAU+0.5
   14   TAU=TAU+0.2
        ITAU=TAU
        IF(ITAU.GT.30) STOP
        GO TO 50
        END
```

TABLE I.

Values for θ/G for various values of non-dimensional time (τ) and non-dimensional location (R): insulated sphere.

$\beta = 0.0$

R \ τ	0.1	0.5	1.0	2.0	5.0	10.0	20.0	120.0 *
1.0	0.0501	0.1320	0.1825	0.2375	0.3085	0.3554	0.3940	0.4943
1.2	0.0408	0.1190	0.1685	0.2228	0.2933	0.3401	0.3786	0.4748
1.4	0.0280	0.0974	0.1441	0.1967	0.2661	0.3125	0.3508	0.4620
1.6	0.0180	0.0761	0.1192	0.1693	0.2369	0.2827	0.3208	0.4340
1.8	0.0114	0.0580	0.0968	0.1438	0.2093	0.2543	0.2921	0.4051
2.0	0.0074	0.0434	0.0776	0.1213	0.1842	0.2283	0.2651	0.3650
2.2	0.0049	0.0322	0.0617	0.1018	0.1618	0.2050	0.2420	0.3500
2.4	0.0034	0.0237	0.0487	0.0851	0.1421	0.1842	0.2207	0.3252
2.6	0.0024	0.0174	0.0383	0.0701	0.1248	0.1657	0.2016	0.3050
2.8	0.0018	0.0128	0.0300	0.0589	0.1096	0.1492	0.1846	0.2852
3.0	0.0013	0.0095	0.0234	0.0489	0.0962	0.1346	0.1693	0.2620
3.4	0.0008	0.0054	0.0143	0.0334	0.0742	0.1097	0.1431	0.2450
3.8	0.0005	0.0032	0.0087	0.0227	0.0571	0.0898	0.1216	0.2225
4.2	0.0003	0.0020	0.0054	0.0154	0.0439	0.0736	0.1039	0.2050
4.6	0.0002	0.0013	0.0034	0.0104	0.0336	0.0604	0.0891	0.1900
5.0	0.0002	0.0009	0.0023	0.0071	0.0258	0.0496	0.0766	0.1720
7.0	0.0000	0.0002	0.0005	0.0012	0.0065	0.0184	0.0369	0.1254
10.0	0.0000	0.0001	0.0001	0.0002	0.0009	0.0039	0.0126	0.0980
15.0	0.0000	0.0000	0.0000	0.0001	0.0002	0.0006	0.0039	0.0540

* Steady State Value

TABLE II.

Values for θ/G for various values of non-dimensional time (τ) and non-dimensional location (R): insulated sphere.

$\beta = 0.1$

R \ τ	0.1	0.5	1.0	2.0	5.0	10.0	15.0	20.0
1.0	0.0499	0.1296	0.1765	0.2241	0.2756	0.2988	0.3058	0.3085
1.2	0.0406	0.1168	0.1627	0.2097	0.2608	0.2840	0.2909	0.2936
1.4	0.0278	0.0953	0.1388	0.1843	0.2346	0.2575	0.2645	0.2671
1.6	0.0179	0.0744	0.1145	0.1578	0.2068	0.2294	0.2363	0.2390
1.8	0.0113	0.0566	0.0926	0.1333	0.1807	0.2030	0.2098	0.2124
2.0	0.0073	0.0423	0.0741	0.1118	0.1573	0.1791	0.1859	0.1885
2.2	0.0049	0.0313	0.0587	0.0934	0.1368	0.1581	0.1648	0.1673
2.4	0.0034	0.0231	0.0463	0.0777	0.1189	0.1397	0.1462	0.1488
2.6	0.0024	0.0170	0.0363	0.0645	0.1034	0.1235	0.1300	0.1325
2.8	0.0018	0.0125	0.0284	0.0534	0.0899	0.1094	0.1157	0.1182
3.0	0.0013	0.0092	0.0222	0.0441	0.0782	0.0970	0.1032	0.1057
3.4	0.0008	0.0052	0.0135	0.0300	0.0592	0.0767	0.0826	0.0850
3.8	0.0005	0.0031	0.0082	0.0201	0.0449	0.0609	0.0665	0.0688
4.2	0.0003	0.0020	0.0137	0.0137	0.0340	0.0485	0.0538	0.0560
4.6	0.0002	0.0013	0.0092	0.0092	0.0258	0.0388	0.0438	0.0459
5.0	0.0002	0.0009	0.0063	0.0063	0.0195	0.0311	0.0357	0.0377
7.0	0.0000	0.0002	0.0011	0.0011	0.0048	0.0105	0.0134	0.0149
10.0	0.0000	0.0001	0.0002	0.0002	0.0007	0.0021	0.0033	0.0039
15.0	0.0000	0.0000	0.0000	0.0000	0.0001	0.0003	0.0007	0.0010

TABLE III.

Values for θ/G for various values of non-dimensional time (τ) and non-dimensional location (R): insulated sphere.

$\beta = 1.0$

R \ τ	0.1	0.5	1.0	2.0	5.0	10.0 *
1.0	0.0479	0.1108	0.1354	0.1489	0.1527	0.1528
1.2	0.0389	0.0989	0.1230	0.1363	0.1400	0.1401
1.4	0.0266	0.0795	0.1023	0.1152	0.1189	0.1190
1.6	0.0171	0.0611	0.0821	0.0943	0.0978	0.0980
1.8	0.0108	0.0458	0.0647	0.0762	0.0796	0.0797
2.0	0.0070	0.0339	0.0504	0.0611	0.0644	0.0644
2.2	0.0046	0.0249	0.0391	0.0488	0.0519	0.0520
2.4	0.0032	0.0182	0.0302	0.0393	0.0419	0.0419
2.6	0.0023	0.0133	0.0233	0.0311	0.0339	0.0339
2.8	0.0017	0.0098	0.0180	0.0249	0.0274	0.0275
3.0	0.0013	0.0072	0.0138	0.0199	0.0222	0.0223
3.4	0.0007	0.0041	0.0083	0.0128	0.0148	0.0148
3.8	0.0005	0.0024	0.0050	0.0083	0.0099	0.0100
4.0	0.0004	0.0019	0.0040	0.0067	0.0082	0.0082
4.5	0.0002	0.0011	0.0023	0.0040	0.0051	0.0051
5.0	0.0002	0.0007	0.0014	0.0024	0.0032	0.0033
7.0	0.0000	0.0001	0.0003	0.0005	0.0007	0.0007
10.0	0.0000	0.0000	0.0001	0.0001	0.0001	0.0001
15.0	0.0000	0.0000	0.0000	0.0000	0.0000	0.0000

* Steady state value

TABLE IV.

Values for θ/G for various values of non-dimensional time (τ) and non-dimensional location (R): insulated sphere.

$\beta = 10.0$

R \ τ	0.1	0.5	1.0 *
1.0	0.0337	0.0433	0.0434
1.2	0.0265	0.0356	0.0357
1.4	0.0175	0.0253	0.0254
1.6	0.0110	0.0172	0.0173
1.8	0.0069	0.0116	0.0116
2.0	0.0045	0.0078	0.0079
2.2	0.0030	0.0054	0.0054
2.4	0.0021	0.0038	0.0038
2.6	0.0015	0.0027	0.0027
2.8	0.0011	0.0019	0.0019
3.0	0.0008	0.0014	0.0014
4.0	0.0003	0.0004	0.0004
7.0	0.0000	0.0000	0.0000

* Steady state value

TABLE V.

Values for θ/θ_0 for various values of non-dimensional time (τ) and non-dimensional location (R); constant temperature sphere.

$\beta = 0.0$

τ R	0.2	0.6	1.0	2.0	5.0	10.6	30.9
1.0	1.0000	1.0000	1.0000	1.0000	1.0000	1.0000	1.0000
1.2	0.6265	0.7126	0.7396	0.7670	0.7913	0.8045	0.8164
1.4	0.3765	0.5107	0.5552	0.6011	0.6424	0.6648	0.6853
1.6	0.2142	0.3649	0.4196	0.4776	0.5309	0.5602	0.5870
1.8	0.1144	0.2584	0.3176	0.3829	0.4446	0.4789	0.5105
2.0	0.0569	0.1806	0.2397	0.3085	0.3759	0.4140	0.4494
2.2	0.0263	0.1242	0.1801	0.2493	0.3202	0.3612	0.3994
2.4	0.0119	0.0839	0.1342	0.2016	0.2741	0.3171	0.3578
2.6	0.0044	0.0554	0.0992	0.1629	0.2357	0.2800	0.3226
2.8	0.0016	0.0358	0.0725	0.1314	0.2033	0.2485	0.2925
3.0	0.0005	0.0226	0.0524	0.1057	0.1757	0.2213	0.2664
3.4	0.0000	0.0084	0.0170	0.0677	0.1215	0.1771	0.2236
4.0	0.0000	0.0015	0.0044	0.0334	0.0766	0.1287	0.1757
5.0	0.0000	0.0001	0.0003	0.0091	0.0345	0.0770	0.1222
8.0	0.0000	0.0000	0.0000	0.0001	0.0021	0.0161	0.0467
20.0	0.0000	0.0000	0.0000	0.0000	0.0000	0.0000	0.0008

TABLE VI.

Values for θ/θ_0 for various values of non-dimensional time (τ) and non-dimensional location (R): constant temperature sphere.

$\beta = 0.1$

R \ τ	0.2	0.6	1.0	2.0	5.0	10.6	30.9
1.0	1.0000	1.0000	1.0000	1.0000	1.0000	1.0000	1.0000
1.2	0.6238	0.7069	0.7319	0.7557	0.7735	0.7799	0.7822
1.4	0.3736	0.5032	0.5444	0.5842	0.6144	0.6254	0.6293
1.6	0.2121	0.3575	0.4081	0.4585	0.4974	0.5117	0.5168
1.8	0.1130	0.2520	0.3066	0.3633	0.4084	0.4251	0.4331
2.0	0.0562	0.1754	0.2300	0.2898	0.3389	0.3575	0.3642
2.2	0.0259	0.1202	0.1718	0.2319	0.2835	0.3035	0.3107
2.4	0.0110	0.0809	0.1275	0.1859	0.2387	0.2597	0.2673
2.6	0.0043	0.0533	0.0938	0.1490	0.2019	0.2236	0.2316
2.8	0.0015	0.0344	0.0683	0.1193	0.1715	0.1936	0.2018
3.0	0.0005	0.0217	0.0492	0.0953	0.1461	0.1683	0.1767
3.4	0.0000	0.0080	0.0246	0.0601	0.1066	0.1287	0.1373
4.0	0.0000	0.0015	0.0079	0.0293	0.0670	0.0877	0.0964
5.0	0.0000	0.0000	0.0009	0.0078	0.0307	0.0478	0.0561
8.0	0.0000	0.0000	0.0000	0.0000	0.0023	0.0081	0.0133
20.0	0.0000	0.0000	0.0000	0.0000	0.0000	0.0000	0.0001

TABLE VII.

Values for θ/θ_0 for various values of non-dimensional time (τ) and non-dimensional location (R): constant temperature sphere.

$\beta = 1.0$

R \ τ	0.2	0.6	1.0	2.0	5.0	10.6 *
1.0	1.0000	1.0000	1.0000	1.0000	1.0000	1.0000
1.2	0.6002	0.6614	0.6740	0.6809	0.6822	0.6823
1.4	0.3491	0.4442	0.4648	0.4764	0.4788	0.4788
1.6	0.1938	0.3000	0.3253	0.3399	0.3429	0.3431
1.8	0.1015	0.2024	0.2297	0.2461	0.2496	0.2496
2.0	0.0498	0.1356	0.1629	0.1801	0.1839	0.1839
2.2	0.0227	0.0899	0.1156	0.1329	0.1368	0.1369
2.4	0.0096	0.0588	0.0820	0.0987	0.1027	0.1027
2.6	0.0037	0.0378	0.0579	0.0736	0.0776	0.0777
2.8	0.0013	0.0239	0.0406	0.0551	0.0590	0.0590
3.0	0.0004	0.0148	0.0283	0.0413	0.0451	0.0451
4.0	0.0000	0.0009	0.0040	0.0098	0.0124	0.0124
8.0	0.0000	0.0000	0.0000	0.0000	0.0001	0.0001

* Steady state value

TABLE VIII.

Values for θ/θ_0 for various values of non-dimensional time (τ) and non-dimensional location (R): constant temperature sphere.

$\beta = 10.0$

τ R	0.2	0.6	1.0 *
1.0	1.0000	1.0000	1.0000
1.2	0.4384	0.4427	0.4427
1.4	0.1951	0.2016	0.2016
1.6	0.0866	0.0937	0.0937
1.8	0.0378	0.0442	0.0443
2.0	0.0160	0.0211	0.0212
2.4	0.0025	0.0049	0.0050
3.0	0.0000	0.0006	0.0006
4.0	0.0000	0.0000	0.0000

* Steady state value

TABLE IX.

Values for θ/G for various values of non-dimensional time (τ) and non-dimensional location (R): insulated cylinder.

$\beta = 0.0$

R \ τ	0.1	0.5	1.0	2.0	5.0	10.0	15.0	20.0
1.0	0.0694	0.2449	0.3985	0.6241	1.0637	1.5190	1.8401	2.0936
1.2	0.0628	0.2342	0.3862	0.6104	1.0475	1.5029	1.8237	2.0770
1.4	0.0517	0.2123	0.3597	0.5780	1.0130	1.4662	1.7861	2.0388
1.6	0.0411	0.1867	0.3274	0.5415	0.9682	1.4181	1.7365	1.9883
1.8	0.0327	0.1664	0.2935	0.4998	0.9182	1.3636	1.6800	1.9307
2.0	0.0263	0.1381	0.2606	0.4576	0.8660	1.3058	1.6198	1.8692
2.2	0.0216	0.1176	0.2298	0.4165	0.8134	1.2468	1.5580	1.8057
2.4	0.0180	0.1000	0.2017	0.3774	0.7615	1.1877	1.4957	1.7416
2.6	0.0152	0.0854	0.1767	0.3409	0.7112	1.1295	1.4338	1.6776
2.8	0.0131	0.0731	0.1543	0.3072	0.6629	1.0724	1.3729	1.6144
3.0	0.0113	0.0631	0.1356	0.2764	0.6168	1.0171	1.3133	1.5524
3.4	0.0088	0.0480	0.1047	0.2232	0.5320	0.9122	1.1990	1.4326
3.8	0.0070	0.0376	0.0821	0.1804	0.4571	0.8157	1.0921	1.3196
4.2	0.0057	0.0301	0.0655	0.1465	0.3919	0.7276	0.9930	1.2137
4.6	0.0048	0.0249	0.0532	0.1198	0.3356	0.6480	0.9015	1.1151
5.0	0.0040	0.0209	0.0442	0.0990	0.2874	0.5762	0.8175	1.0235
7.0	0.0020	0.0104	0.0213	0.0453	0.1372	0.3186	0.4964	0.6616
10.0	0.0010	0.0051	0.0102	0.0209	0.0576	0.1398	0.2404	0.3496
15.0	0.0005	0.0024	0.0049	0.0104	0.0290	0.0688	0.1233	0.1945

TABLE X.

Values for θ/G for various values of non-dimensional time (τ) and non-dimensional location (R): insulated cylinder.

$\beta = 0.1$

τ	0.1	0.5	1.0	2.0	5.0	10.0	15.0	20.0
R								
1.0	0.0690	0.2396	0.3823	0.5771	0.8913	1.1131	1.2072	1.2521
1.2	0.0625	0.2290	0.3702	0.5637	0.8769	1.0983	1.1922	1.2371
1.4	0.0514	0.2074	0.3444	0.5345	0.8446	1.0650	1.1586	1.2034
1.6	0.0409	0.1823	0.3129	0.4977	0.8033	1.0219	1.1152	1.1598
1.8	0.0325	0.1575	0.2801	0.4582	0.7576	0.9741	1.0667	1.1111
2.0	0.0262	0.1347	0.2483	0.4184	0.7105	0.9242	1.0162	1.0603
2.2	0.0214	0.1146	0.2187	0.3798	0.6636	0.8741	0.9652	1.0091
2.4	0.0179	0.0975	0.1919	0.3434	0.6179	0.8248	0.9150	0.9585
2.6	0.0152	0.0832	0.1679	0.3095	0.5739	0.7769	0.8660	0.9092
2.8	0.0130	0.0713	0.1469	0.2784	0.5322	0.7308	0.8188	0.8616
3.0	0.0113	0.0615	0.1287	0.2500	0.4928	0.6868	0.7735	0.8159
3.4	0.0088	0.0467	0.0993	0.2014	0.4212	0.6053	0.6892	0.7306
3.8	0.0070	0.0366	0.0778	0.1625	0.3591	0.5325	0.6133	0.6536
4.2	0.0057	0.0295	0.0621	0.1318	0.3059	0.4679	0.5455	0.5846
4.6	0.0047	0.0243	0.0506	0.1078	0.2605	0.4111	0.4851	0.5229
5.0	0.0040	0.0204	0.0420	0.0891	0.2222	0.3611	0.4316	0.4680
7.0	0.0020	0.0102	0.0203	0.0409	0.1054	0.1918	0.2435	0.2726
10.0	0.0010	0.0049	0.0097	0.0189	0.0447	0.0835	0.1124	0.1316
15.0	0.0004	0.0023	0.0047	0.0094	0.0225	0.0413	0.0568	0.0690

TABLE XI.

Values for θ/G for various values of non-dimensional time (τ) and non-dimensional location (R): insulated cylinder.

$\beta = 1.0$

R \ τ	0.1	0.5	1.0	2.0	5.0	10.0 *
1.0	0.0661	0.1988	0.2729	0.3269	0.3480	0.3487
1.2	0.0598	0.1892	0.2626	0.3162	0.3372	0.3379
1.4	0.0491	0.1701	0.2412	0.2938	0.3147	0.3154
1.6	0.0390	0.1484	0.2162	0.2673	0.2877	0.2884
1.8	0.0310	0.1273	0.1909	0.2400	0.2601	0.2607
2.0	0.0249	0.1083	0.1672	0.2140	0.2334	0.2341
2.2	0.0204	0.0919	0.1456	0.1899	0.2087	0.2094
2.4	0.0171	0.0780	0.1266	0.1682	0.1863	0.1869
2.6	0.0145	0.0664	0.1100	0.1488	0.1661	0.1668
2.8	0.0124	0.0569	0.0958	0.1316	0.1482	0.1488
3.0	0.0108	0.0490	0.0836	0.1166	0.1323	0.1329
3.4	0.0084	0.0373	0.0643	0.0919	0.1060	0.1065
3.8	0.0067	0.0293	0.0504	0.0732	0.0856	0.0861
4.2	0.0054	0.0236	0.0403	0.0590	0.0698	0.0703
4.6	0.0045	0.0195	0.0329	0.0482	0.0575	0.0580
5.0	0.0038	0.0163	0.0274	0.0400	0.0480	0.0484
7.0	0.0019	0.0082	0.0134	0.0819	0.0226	0.0228
10.0	0.0010	0.0040	0.0064	0.0089	0.0104	0.0105
15.0	0.0004	0.0019	0.0031	0.0043	0.0051	0.0052

* Steady state value

TABLE XII.

Values for θ/G for various values of non-dimensional time (τ) and non-dimensional location (R): insulated cylinder.

$\beta = 10.0$

R \ τ	0.1	0.5	1.0 *
1.0	0.0449	0.0633	0.0656
1.2	0.0400	0.0578	0.0581
1.4	0.0323	0.0487	0.0490
1.6	0.0255	0.0399	0.0402
1.8	0.0208	0.0326	0.0328
2.0	0.0163	0.0267	0.0269
2.2	0.0133	0.0221	0.0222
2.4	0.0111	0.0184	0.0186
2.6	0.0094	0.0156	0.0158
2.8	0.0081	0.0133	0.0135
3.0	0.0071	0.0116	0.0117
3.4	0.0055	0.0089	0.0090
3.8	0.0044	0.0071	0.0071
4.2	0.0036	0.0058	0.0058
4.6	0.0030	0.0048	0.0048
5.0	0.0025	0.0040	0.0041
7.0	0.0013	0.0020	0.0021
10.0	0.0006	0.0010	0.0010
15.0	0.0003	0.0005	0.0005

* Steady state value

TABLE XIII.

Values for θ/θ_0 for various values of non-dimensional time (τ) and non-dimensional location (R): constant temperature cylinder.

$\beta = 0.0$

R \ τ	0.1	0.5	1.0	2.0	5.0	10.0	15.0	20.0
1.0	1.0000	1.0000	1.0000	1.0000	1.0000	1.0000	1.0000	1.0000
1.2	0.6091	0.7771	0.8214	0.8543	0.8856	0.9027	0.9108	0.9159
1.4	0.3266	0.5939	0.6724	0.7319	0.7890	0.8205	0.8355	0.8449
1.6	0.1510	0.4448	0.5469	0.6273	0.7058	0.7494	0.7703	0.7834
1.8	0.0590	0.3254	0.4412	0.5368	0.6329	0.6870	0.7129	0.7292
2.0	0.0190	0.2319	0.3524	0.4583	0.5683	0.6313	0.6617	0.6809
2.2	0.0050	0.1608	0.2783	0.3898	0.5107	0.5813	0.6156	0.6372
2.4	0.0010	0.1083	0.2171	0.3302	0.4590	0.5360	0.5737	0.5976
2.6	0.0001	0.0707	0.1672	0.2784	0.4123	0.4947	0.5354	0.5612
2.8	0.0000	0.0447	0.1270	0.2334	0.3702	0.4569	0.5001	0.5277
3.0	0.0000	0.0273	0.0951	0.1946	0.3320	0.4221	0.4676	0.4967
3.4	0.0000	0.0092	0.0509	0.1327	0.2659	0.3604	0.4093	0.4412
3.8	0.0000	0.0027	0.0256	0.0881	0.2115	0.3075	0.3588	0.3924
4.2	0.0000	0.0007	0.0120	0.0569	0.1669	0.2618	0.3145	0.3495
4.6	0.0000	0.0001	0.0053	0.0356	0.1306	0.2224	0.2755	0.3114
5.0	0.0000	0.0000	0.0022	0.0216	0.1011	0.1883	0.2411	0.2774
7.0	0.0000	0.0000	0.0000	0.0011	0.0239	0.0770	0.1200	0.1534
10.0	0.0000	0.0000	0.0000	0.0000	0.0015	0.0157	0.0368	0.0586
15.0	0.0000	0.0000	0.0000	0.0000	0.0000	0.0010	0.0066	0.0173

TABLE XIV.

Values for θ/θ_0 for various values of non-dimensional time (τ) and non-dimensional location (R): constant temperature cylinder.

$\beta = 0.1$

R \ τ	0.1	0.5	1.0	2.0	5.0	10.0	15.0	20.0
1.0	1.0000	1.0000	1.0000	1.0000	1.0000	1.0000	1.0000	1.0000
1.2	0.6072	0.7713	0.8126	0.8412	0.8669	0.8725	0.8749	0.8758
1.4	0.3249	0.5859	0.6590	0.7106	0.7576	0.7679	0.7724	0.7740
1.6	0.1500	0.4365	0.5316	0.6013	0.6659	0.6803	0.6864	0.6888
1.8	0.0585	0.3180	0.4258	0.5087	0.5877	0.6056	0.6132	0.6162
2.0	0.0188	0.2259	0.3379	0.4297	0.5203	0.5411	0.5501	0.5536
2.2	0.0049	0.1561	0.2654	0.3620	0.4617	0.4850	0.4952	0.4990
2.4	0.0010	0.1048	0.2060	0.3040	0.4103	0.4350	0.4470	0.4512
2.6	0.0001	0.0683	0.1580	0.2542	0.3650	0.3923	0.4044	0.4090
2.8	0.0000	0.0431	0.1195	0.2115	0.3249	0.3537	0.3665	0.3714
3.0	0.0000	0.0262	0.0892	0.1752	0.2893	0.3193	0.3328	0.3380
3.4	0.0000	0.0088	0.0475	0.1180	0.2293	0.2609	0.2754	0.2811
3.8	0.0000	0.0026	0.0238	0.0776	0.1814	0.2137	0.2289	0.2349
5.0	0.0000	0.0000	0.0020	0.0186	0.0876	0.1176	0.1332	0.1397
7.0	0.0000	0.0000	0.0000	0.0009	0.0228	0.0420	0.0546	0.0606
15.0	0.0000	0.0000	0.0000	0.0000	0.0000	0.0004	0.0020	0.0038

TABLE XV.

Values for θ/θ_0 for various values of non-dimensional time (τ) and non-dimensional location (R): constant temperature cylinder.

$\beta = 1.0$

R \ τ	0.1	0.5	1.0	2.0	5.0 *
1.0	1.0000	1.0000	1.0000	1.0000	1.0000
1.2	0.5908	0.7246	0.7466	0.7549	0.7566
1.4	0.3102	0.5220	0.5607	0.5757	0.5789
1.6	0.1414	0.3716	0.4221	0.4422	0.4466
1.8	0.0547	0.2604	0.3175	0.3414	0.3467
2.0	0.0175	0.1790	0.2381	0.2645	0.2706
2.2	0.0045	0.1203	0.1778	0.2054	0.2121
2.4	0.0009	0.0789	0.1319	0.1598	0.1668
2.6	0.0001	0.0504	0.0970	0.1243	0.1316
2.8	0.0000	0.0312	0.0708	0.0967	0.1040
3.0	0.0000	0.0188	0.0511	0.0752	0.0825
3.4	0.0000	0.0061	0.0257	0.0452	0.0521
3.8	0.0000	0.0018	0.0123	0.0269	0.0331
5.0	0.0000	0.0000	0.0009	0.0051	0.0086
7.0	0.0000	0.0000	0.0000	0.0002	0.0009
15.0	0.0000	0.0000	0.0000	0.0000	0.0000

* Steady state value

TABLE XVI.

Values for θ/θ_0 for various values of non-dimensional time (τ) and non-dimensional location (R): constant temperature cylinder.

$\beta = 10.0$

τ	0.1	0.5	1.0 *
R			
1.0	1.0000	1.0000	1.0000
1.2	0.4631	0.4889	0.4890
1.4	0.2028	0.2421	0.2421
1.6	0.0809	0.1208	0.1210
1.8	0.0284	0.0607	0.0609
2.0	0.0085	0.0306	0.0308
2.2	0.0021	0.0155	0.0157
2.4	0.0004	0.0078	0.0080
2.6	0.0000	0.0039	0.0041
2.8	0.0000	0.0020	0.0021
3.0	0.0000	0.0010	0.0010
3.4	0.0000	0.0002	0.0003
3.8	0.0000	0.0001	0.0001

* Steady state value

BIBLIOGRAPHY

1. Alberts, W. W., Wright, E. W., "A Thermistor Brain Probe," J. Neurosurg., Vol 18, 1961, p. 560.

2. Alberts, W. W., Wright, E. W., Feinstein, B., and Von Bonin, G., "Experimental Radio-Frequency Brain Lesion Size as a Function of Physical Parameters," J. Neurosurg., Vol 25, 1966, pp. 421-23.

3. Aronow, S., "The Use of Radio-Frequency Power in Making Lesions in the Brain," J. Neurosurg., May 1960, pp. 431-438.

4. Borison, H. L., Wang, S. W., "Quantitative Effects of Radon Implanted in the Medulla Oblangata: A Technique for Producing Discrete Lesions," J. Comp. Neur., Vol 94, 1951, pp. 35-55.

5. Brodkey, J. S., Miyazaki, Y., Ervin, F. R., and Mark, V. H., "Reversible Heat Lesions with Radiofrequency Current," J. Neurosurg., Vol 21, 1964, pp. 49-53.

6. Carpenter, M., Whittier, J. R., "Study of Methods for Producing Experimental Lesions of the Central Nervous System with Special Reference to Stereotaxic Technique," J. of Comp. Neurology, Vol 97, 1952, pp. 73-117.

7. Carslaw, H. S., and Jaeger, J. C., Conduction of Heat in Solids, 2nd Ed., Exford University Press, 1959.

8. Crandall, S. H., Engineering Analysis, pp. 171-173, McGraw Hill, 1956.

9. Cooper, I. S., Gionino, G., Terry, R., "The Cryogenic Lesion," Confin. Neurol., Vol 26, 1965, pp. 161-177.

10. Cooper, T. E. and Trezek, G. J., "Analytical Prediction of the Temperature Field Emanating From a Cryogenic Surgical Cannula," Cryobiology, Vol 7, No. 2-3, 1970, pp. 79-93.

11. Cooper, T. E. and Trezek, G. J., "Correlation of Thermal Properties of Some Human Tissue with Water Current," Aerospace Med., Vol 42, 1971, pp. 24-27.

12. Cooper, T. E. and Trezek, G. J., "Rate of Lesions Growth Around Spherical and Cylindrical Cryoprobes," Cryobiology, Vol 7, No. 4-6, 1971, pp. 183-190.

13. Dieckmann, G., Gabriel, E., and Hassler, R., "Size, Form and Structural Peculiarities of Experimental Brain Lesions Obtained by Thermocontrolled Radio-frequency," Confinia Neurol., Vol 26, 1965, pp. 134-142.

14. Feinstein, B., Alberts, W., and Wright, E., "Implantable Thermistor Electrodes for RF Lesion Production," J. Neurosurg., Vol 30, 1969, pp. 313-314.

15. Galton, L., "Sub-Zero Surgery," Family Circle, March 1968.

16. Gildenberg, P. L., "Pattern of Brain Heating Studied with a High-Resistance Heating Electrode," Confinia Neurologica, Vol 22, 1962, pp. 343-345.

17. Glees, P., Wall, P. D., Wright, T. A., "An Ensheathed Rotating Knife for Causing Brain Lesions," Nature, Vol 160, 1947, p. 365.

18. Herrero, S., "Radio-Frequency-Current and Direct-Current Lesions in the Ventromedial Hypothalamus," Americal Journal of Physiology, Vol 217, No. 2, August 1969, pp. 403-410.

19. Letcher, F. S., Goldring, S., "The Effect of Radio-frequency Current and Heat on Peripheral Nerve Action Potential in the Cat," J. Neurosurg., Vol 29, 1968, pp. 42-47.

20. Lynn, J., Zwemmer, R. L., Chick, A. J. and Miller, A. E., "A New Method for the Generation and Use of Focused Ultrasound in Experimental Biology," J. Gen. Physiol., Vol 26, 1942, pp. 179-193.

21. Mark, V. H., Chiba, T., Ervin, F. R., and Hamlin, H., "The Comparison of Heat and Cold for the Production of Localized Lesions in the Central Nervous System," Confinia Neurol, Vol 26, 1965, pp. 178-184.

22. Mullan, S., Mailis, M., Karasick, J., Vailati, G., and Beckman, F., "A Reappraisal of the Unipolar Anodal Electrolytic Lesion, J. Neurosurg., Vol 22, 1965, pp. 531-538.

23. Ozisik, M. N., Boundary Value Problems of Heat Conduction, CN 9, International Textbook Company, 1968.

24. Perl, W., "Heat and Matter Distribution in Body Tissue and the Determination of Tissue Blood Flow by Local Clearance Methods," J. Theoret. Biol., Vol 2, 1962, pp. 201-235.

25. Perl, W., and Hirsch, R. L., "Local Blood Flow in Kidney Tissue by Heat Clearance Measurement," J. Theor. Biol., Vol 10, 1966, pp. 251-280.

26. Petty, P. G., and Edsall, G., "Alternating - Current Electrocoagulation with Bipolar Electrodes," J. Neurosurg., Vol 26, 1967, pp. 399-405.

27. Rosomoff, H. L. and Holaday, D. A., "Cerebral Blood Flow and Cerebral Oxygen Consumption During Hypothermia," Amer. J. Physiol., Vol 179, 1954, pp. 85-88.

28. Rowland, V., MacIntyre, W. J., and Bidder, T. G., "The Production of Brain Lesions with Electric Currents, II Bidirectional Currents," J. Neurosurg., January 1960, pp. 55-69.

29. Rutkin, B. and Barish, E., Localized Thermal Distributions in Brain, paper presented at 17th Annual Conference on Engineering in Medicine and Biology, Cleveland, November 1964.

30. Sarby, B., Wennerstrand, J., and Del Corral-Gutierrez, J., "Some Observations on Stereotaxic Radiofrequency and Photon Beam Lesions," Confinia Neurol., Vol 26, 1965, p. 133.

31. Sias, F. R. and Goodman, D. C., "A Constant Radio-Frequency Coagulator for Producing Lesions in Nervous Tissue," Amer. J. Med. Electronics, Vol 2, 1963, pp. 239-242.

32. Spector, H., "A Thermode-Electrode for Physiological Studies of Highly Discrete Tissue Loci," J. Applied Physiology, Vol 27, No. 5, November 1969, pp. 770-773.

33. Stein, S. N. and Peterson, E. W., "The Use of Radon Seeds to Produce Deep Cerebral Lesions," Proc. Soc. Exp. Biol. and Med., Vol 74, 1950, pp. 583-585.

34. Szekely, E. G., Egyed, J. J., Jacoby, C. G., Moffet, R., Spiegal, E. A., "High Frequency Coagulation by Means of a Stylet Electrode Under Temperature Control," Confinia Neurol., Vol 26, 1965, pp. 146-152.

35. Van Den Berg, J. and Van Manen, B., "Graded Coagulation of Brain Tissue," Acta Physiol. Parmacol. Neerlandia, Vol 10, 1962, pp. 353-357.

36. Von Bonin, G., Alberts, W., Wright, E., and Feinstein, B., "Radiofrequency Brain Lesions," Archives of Neurology, Vol 12, January 1965, pp. 25-29.

37. Watkins, E. S., "Heat Gains in Brain During Electrocoagulative Lesions," J. Neurosurg., Vol 23, 1965, pp. 319-328.

38. Wood, R. W., Loomis, A. L., "The Physical and Biological Effects of High Frequency Sound-Waves of Great Intensity," Philosophical Magazine and Journal of Science, S.7, Vol 4, No. 22, September 1927, pp. 417-436.

39. Zervas, N. T., "Technique of Radio-Frequency Hypophysectomy," Confinia Neurol., Vol 26, 1965, pp. 157-160.

INITIAL DISTRIBUTION LIST

		No. Copies
1.	Defense Documentation Center Cameron Station Alexandria, Virginia 22314	2
2.	Library, Code 0212 Naval Postgraduate School Monterey, California 93940	2
3.	Asst Professor T. E. Cooper, Code 59Cg Department of Mechanical Engineering Naval Postgraduate School Monterey, California 93940	3
4.	ENS Patrick L. Gengler, USN 1919 East Bennett Avenue Milwaukee, Wisconsin 53207	1
5.	Thesis Office, Attn: M. Burton Naval Postgraduate School Monterey, California 93940	1

UNCLASSIFIED
Security Classification

DOCUMENT CONTROL DATA - R & D

(Security classification of title, body of abstract and indexing annotation must be entered when the overall report is classified)

1 ORIGINATING ACTIVITY (Corporate author)

Naval Postgraduate School
Monterey, California 93940

2a. REPORT SECURITY CLASSIFICATION

UNCLASSIFIED

2b. GROUP

3 REPORT TITLE

HEAT TRANSFER ANALYSIS OF A RADIO-FREQUENCY BRAIN PROBE

4 DESCRIPTIVE NOTES (Type of report and inclusive dates)

Master's Thesis, June 1971

5. AUTHOR(S) (First name, middle initial, last name)

Patrick L. Gengler

6. REPORT DATE	7a. TOTAL NO. OF PAGES	7b. NO. OF REFS
June 1971	114	39

8a. CONTRACT OR GRANT NO.	9a. ORIGINATOR'S REPORT NUMBER(S)
b. PROJECT NO.	
c.	9b. OTHER REPORT NO(S) (Any other numbers that may be assigned this report)
d.	

10 DISTRIBUTION STATEMENT

Approved for public release; distribution unlimited.

11. SUPPLEMENTARY NOTES	12. SPONSORING MILITARY ACTIVITY
	Naval Postgraduate School Monterey, California 93940

13. ABSTRACT

This analysis is concerned with the use of radio-frequency (rf) current in producing lesions in the brain. The technique consists of passing the current between an active electrode implanted in the brain and an indifferent electrode located in the skull. The resistivity of the tissue causes electrical energy to be converted into heat thus raising the tissue temperature. A problem that is sometimes encountered is uncontrollable boiling of the tissue near the probe tip. A theoretical model which considers the combined effects of conduction, blood flow, metabolism, and rf heating is presented to show the relative effects of each of the terms on the temperature field. It was found that conductive effects and rf heating effects are very important parameters in predicting lesion size, while the blood flow effect is only marginally important. It is proposed that by maintaining the temperature of the probe at a low constant value, the maximum temperature of the lesion can be kept well below the boiling point, yet because currents and time can be increased, the volume of tissue destroyed equals or even surpasses that of the conventional probe. Finally, the radio-frequency probes are compared to resistively heated probes. The lesions produced by these probes are shown to be significantly smaller than the lesions produced by the rf probes.

DD FORM 1 NOV 65 1473 (PAGE 1)

S/N 0101-807-6811

UNCLASSIFIED
Security Classification

KEY WORDS	LINK A		LINK B		LINK C	
	ROLE	WT	ROLE	WT	ROLE	WT
Radio Frequency Heating						
Brain Probe						
Heat Transfer						
Conduction						
Blood Flow						
Surgery						